678

PROPOSAL TO STUDY THE SPIN DEPENDENCE IN INCLUSIVE π° AND DIRECT GAMMA PRODUCTION AT HIGH P_T WITH THE POLARIZED PROTON BEAM FACILITY AT FERMILAB

by

D. Hill, H. Spinka, R. Stanek, K. Toshioka, D. Underwood, and A. Yokosawa
Argonne National Laboratory, Argonne, Illinois

Y. Hemmi, K. Imai, R. Kikuchi, K. Miyake, T. Nakamura,
K. Nishimura and N. Tamura
Kyoto University, Kyoto, Japan

H. Azaïez, K. Kuroda, A. Michalowicz, D. Perret-Gallix
LAPP, Annecy, France

G. Shapiro
Lawrence Berkeley Laboraotry
University of California, Berkeley, California

D. H. Miller and C. LeRoy
Northwestern University, Evanston, Illinois

M. Corcoran, H. E. Miettinen, T. A. Mulera, G. S. Mutchler,
G. C. Phillips and J. B. Roberts
Rice University, Houston, Texas

J. Bistrisky, A. DeLesquen, F. Lehar, and L. Van Rossum
Saclay, France

V. Apokin, Y. Matulenko, A. Meschanin, S. Nurushev,
V. Solovyanov and A. Vasilyev
Serpukhov, USSR

R. Birsa, F. Bradamante, S. Dalla Torre-Colautti, M. Giorgi, L. Lanceri,
A. Martin, P. Moras, A. Penzo, P. Schiavon and A. Villari
INFN, Sezione di Trieste, Trieste, Italy

January 25, 1981

Scientific Spokesman:
K. Kuroda
LAPP, Annecy, France
Telephone: (50)-23-32-45

ABSTRACT

We propose to measure the single-spin asymmetry parameter A_N in inclusive π^o production and direct-γ production at high p_T using the polarized proton-beam facility at Fermilab. In addition, we propose to measure the double-spin asymmetry parameter A_{LL} in inclusive π^o production using a polarized proton target. The measurement of A_{LL} will be extended to direct-γ production when improved target materials become available.

I. INTRODUCTION

Investigation of the substructure of hadrons and the behavior of hadronic constituents is presently among the most active areas of high energy physics. Recent data on deep-inelastic ep scattering [1)2)] are most directly interpreted as evidence that quarks at large-X have high probability for retaining the helicity of the parent proton. Since high-p_T hadron or photon production results predominantly from the hard scattering of hadronic constituents it is reasonable to expect that spin dependence in these fundamental subprocesses can be further investigated using polarized protons [3)4)5)].

We propose to study spin dependence in the reactions

$$p + p \rightarrow \pi^o + \text{anything}, \quad \text{and} \tag{1}$$

$$p + p \rightarrow \gamma + \text{anything} \tag{2}$$

with emphasis on the high-p_T region. The quantities to be measured are the single-spin asymmetries

$$A_N = \frac{Ed^3\sigma(\uparrow)/dp^3 - Ed^3\sigma(\downarrow)/dp^3}{Ed^3\sigma(\uparrow)/dp^3 + Ed^3\sigma(\downarrow)/dp^3} \tag{3}$$

for both reactions (1) and (2) with a transversely polarized proton beam and liquid hydrogen (H_2) target. In addition we propose to measure the double-spin asymmetry in reaction (1)

$$A_{LL} = \frac{Ed^3\sigma(++)/dp^3 - Ed^3\sigma(+-)/dp^3}{Ed^3\sigma(++)/dp^3 + Ed^3\sigma(+-)/dp^3} \tag{4}$$

where ++(+-) indicate parallel (antiparallel) helicities for longitudinally polarized beam and target protons. This measurement requires replacement of the liquid H_2 target by a polarized proton target (PPT).

II. PHYSICS MOTIVATION

The single-spin asymmetries in reactions (1) and (2) are expected to be close to zero in current QCD theory even with higher order corrections ($A_N \simeq O(m_q/\sqrt{s})$ where m_q is the mass of the light quark). Nevertheless, large asymmetries in inclusive π^o production have been observed at the CERN PS[6] for $p_{in} = 24$ GeV/c, $X_F \simeq 0$, and $1.0 < p_T < 2.5$ GeV/c. Although this kinematic region may be too low to contradict directly the validity of the constituent model based on QCD these results provide strong motivation for extending similar measurements to regions of higher p_{in} and p_T. The high-intensity polarized-proton facility to be constructed at Fermilab[7] can usefully cover the p_T region to 4-5 GeV/c at $p_{in} = 300$ GeV/c for both reaction (1) and (2). If large asymmetries are observed at such large p_T they would present a serious challenge to the attractive model of hard scattering and perturbative QCD.

The QCD Compton effect, gluon + quark $\rightarrow$ gamma + quark, is expected to be the dominant mechanism for direct-γ production at large p_T. In contrast to the π^o which represents only a fragment of the scattered constituent the γ itself participates directly in the hard-scattering process. As a direct consequence the ratio γ/π^o should increase with increasing p_T; this prediction has recently been confirmed in several different experiments[8][9][10]. Thus, direct-γ production provides a particularly clean process for studying the dynamics of hadronic constituents without the complexities of quark fragmentation. We emphasize that on the experimental side the use of a polarized beam on a liquid H_2 target provides a particularly clean technique for studying single-spin asymmetries without the complexity of polarized targets and the unavoidable background from production on unpolarized constituents therein.

Although important qualitative features may be deduced from single-spin asymmetry measurements, the study of double-spin asymmetries can provide quantitative insight into the spin properties of gluons which are not accessible to deep-inelastic ep scattering experiments. The double-spin asymmetry A_{LL} in inclusive π^o production has been estimated by several authors; their results are shown in Fig. 6. Curve (a) was obtained by Babcock et al.[3] using a hard-scattering model based on QCD perturbation theory; although the predicted asymmetry is small it has a definite positive sign. Cheng and Fischbach[5)] predict a much larger asymmetry using the effective-gluon model (E-G); Sivers et al.[11)] find zero asymmetry in the constituent interchange model (CIM). The large differences are a consequence of the different spin dependences assumed in the fundamental subprocesses for these models; the present experient will be sufficiently sensitive to discriminate among these models.

The double-spin asymmetry for direct-γ production has recently been estimated by Hidaka[12)] assuming QCD Compton and $q\bar{q}$ annihilation as dominant subprocesses. These same assumptions successfully describe available data for the unpolarized cross sections. His results suggest significant asymmetries at large X_T ($\simeq 5\%$ at $X_F \simeq 0$ and $X_T \simeq 0.5$). Because of the polarization dilution in available polarized proton targets A_{LL} cannot yet be measured with adequate precision; however, targets of sufficient spin purity are under development at Saclay and CERN. Because of the importance of direct-γ production as a hadronic probe we propose to extend the double-spin measurements to this final state when improved target materials become available.

III. EXPERIMENTAL METHODS

a) Experimental Arrangement

A schematic view of the experimental arrangement is shown in Fig.1. The polarized proton beam to be constructed in the M2 beam line[7)] enters from the left. Trajectories of individual beam particles are defined by hodoscopes H_1 and H_2; these are separated by 20 meters and have spatial resolutions of 1.5 mm in both the x and y directions. For single-spin measurements a liquid H_2 target 100 cm long will be used with the proton beam transversely polarized. For the double-spin asymmetry measurements the longitudinally polarized proton beam will be incident on a longitudinally polarized proton target. The proposed snake system will allow the beam polarization to be flipped from spill to spill with no important change in beam geometry.

Gammas produced by the interaction of protons on either target are detected in the two Pb-glass spectrometers $G_1$and G_2. At $p_{in} = 300$ GeV/c the spectrometers are placed 12 m downstream of the target and centered around $\Theta = 80$ mrad which corresponds to $X_F = 0$. The azimuthal angle subtended by each spectrometer is $\pm 22.5^{\circ}$ with respect to the horizontal plane.

The scintillation hodoscopes H_3 and H_4, immediately in front of the Pb-glass spectrometers, are constructed in three planes for segmentation in the X, Y, and U directions; these have spatial resolutions of 4 cm and serve to localize charged particles which accompany γ's. To improve background identification in direct-γ production each Pb-glass spectrometer is provided with a guard counter G_1' and G_2'. These coarse-grained Cerenkov shower counters ensure identification of π^o and η^o decays in which only one γ falls within the fiducial area of a Pb-glass spectrometer.

The acceptance of the detector in X_F-p_T space is shown in Fig. 2 for p_{in} = 300 GeV/c.

b. Gamma Spectrometers

The two gamma spectrometers comprise the major part of the detector. Each consists of 372 Pb-glass cells (3.8x3.8x45 cm) stacked to form a trapezoidal array as shown in Fig. 3. The Cerenkov light is collected by a photomultiplier at the rear of each cell. The detector elements and the design of the associated electronic system will be similar to those developed by the IHEP-IFSN-LAPP Collaboration for the GAMS 4000 spectrometer[13) at CERN. The principal characteristics of this spectrometer are listed in Table 1.

The remarkable spatial resolution of the GAMS spectrometer (±1 mm at 200 GeV) results from an optimal choice of transverse dimension 2Δ of the Pb-glass cells[14)]. By choosing Δ just slightly smaller than the effective half-width (2 cm for Pb-glass of type F-8) of an electromagnetic shower it spreads over only a few cells to form a cluster. A fit to the energy deposition pattern in the cluster provides the position coordinates for the incident γ. The ability to resolve the merged clusters produced by two close γ's is particularly important for efficient identification of direct-γ's in a background of π^o decays. The IHEP group has found experimentally[15)] that pairs of γ's from π^o decay can be discriminated from single γ's for transverse separations greater than 2.5 cm even when both γ's fall within the same cell of the spectrometer.

Geometric efficiencies for π^o detection have been studied using Monte Carlo simulation; results are shown in Fig. 4 for a kinematic region around X_F = 0. With increasing p_T the probability for detecting both γ's from a π^o decay (solid circles) asymptotically approaches the

25% azimuthal angle subtended by the spectrometers ($2x45^{o}$). At lower p_T the efficiency decreases as the probability for one of the γ's to miss a spectrometer increases. For $X_F = 0$ the probability that only a single γ falls within the detector acceptance (triangle points) decreases rapidly with increasing p_T. For $X_F \neq 0$ the π^o angle varies rapidly with p_T; this results in a maximum near $p_T = 4$ GeV/c for the probability that a single γ falls within the detector acceptance. The probability that both γ's from a π^o decay fall within a single cell (open circles) is almost negligible for $p_T < 7$ GeV/c. Even so, many of these events will be resolved since the transverse separation of the two γ's will be larger than the discrimination limit of 2.5 cm.

To accommodate high event rates the integrated charge in each cell is digitized with its own ADC. Pedestal subtraction and energy normalization are performed automatically by a fast processor. Relative gains (PM + ADC) will be monitored under microprocessor control with an LED system between spills to achieve a long-term stability better than 1%. The energy resolution has been measured for a spectrometer of this type; at full width half-maximum (FWHM) it is

$$\Delta E/E = 0.025 + 0.13/\sqrt{E}(\mathrm{GeV})$$

giving ± 2.5% at 25 GeV. Linearity has been studied with electrons from 1-4 GeV by the EHS group at CERN and from 1.8-40 GeV by the GAMS group at IHEP. No deviation larger than 1% was observed.

Energies and coordinates (using the method of moments) will be evaluated on-line. This provides the possibility for imposing event selection criteria if necessary before recording data on tape. With reasonable estimates for processing times we conclude that as many as 500 events/sec can be recorded even with large multiplicities.

c. Identification of π^o Events

Fast discriminators sample the integrated charge in each cell. Thresholds are adjusted so that the detector is triggered when an energy greater than 10 GeV is deposited in any cell. This allows efficient detection of π^o's emitted near $X_F \simeq 0$ and $p_T < 2.0$ GeV/c. If rates are too high the discriminator thresholds can be increased or the hodoscopes H_3 and H_4 can be used to reject clusters associated with charged particles. It is apparent, however, that event reject is preferably executed off-line after careful study so that no bias is introduced in the inclusive final states.

To obtain a 'clean' sample of π^0 events all data must be subjected to extensive off-line analysis. Backgrounds due to improperly paired γ's will be estimated using Monte Carlo simulation with reconstructed π^0's as input. Contamination of the final sample by π^0's from decay of inclusively produced η^0's, ω^0's, and K_s^0's can be reasonably estimated from available measurements and models which relate charged and neutral production. This contamination will be small at high p_T.

d. Identification of Direct-γ Events

The problems involved in identification of direct-γ 's in a background of π^0 decays have recently been addressed with considerable success by several groups[8)9)10)]. Background arises from

i) The decays $\pi^0 \to \gamma\gamma$ and $\eta^0 \to \gamma\gamma$ in which one γ misses a spectrometer, is below threshold for detection, or converts in the target; or the two γ's are too closely spaced to be geometrially resolved; and

ii) Neutral hadrons such as n, $\bar{n}$, or K_L^0 which interact in the Pb-glass and simulate a single shower.

We propose to surround the Pb-glass spectrometers with gaurd counters to detect γ's which otherwise would be lost. With Monte Carlo simulation we find that a lateral thickness of 30 cm is enough to detect 97% of these associated γ's arising from decay of π^0's emitted near $X_F = 0$ with $p_T \simeq 5$ GeV/c. Because of the large volume (0.5 m^3) and complex shape of the gaurd counters we propose to use a water solution of heavy elements (for example ZnI, with $\rho \simeq 2.8$, and R.L. $\simeq$ 4.2 cm) as recently developed at KEK[16)]. The direct measurement of this important background will result in significant improvement of the final error compared with the alternative of subtracting background with Monte Carlo simulation. The background from unresolved π^0 decays is very small. Less than 0.3% of all π^0decays falling within the detector acceptance are unresolved for $p_T \simeq 6$ GeV/c; for $\gamma/\pi^0 \simeq 0.1$ this represents only a 3% background for direct-γ's. The background from conversions in the target can be reliably estimated from the reconstructed π^0 events.

The neutral hadron contribution to background will be measured in a separate run using the method of Cox et al.[10)]. Ten radiation lengths of Pb will be inserted in the space between the hodoscopes H_3 and H_4 and the Pb-glass spectrometers. The γ flux is largely degraded while the neutral hadronic component is attenuated only 30% due to interactions in the Pb. This background varies from 10 to 40% depending on the kinematic region and therefore must be subtracted separately in each X_F and p_T interval.

Measurement of single-spin asymmetries will be carried out simultaneously for the inclusive π^o's and direct-γ's.

IV. RATE AND ERROR ESTIMATES

Rates for π^o production have been estimated with the following assumptions:

p_{in} = 300 GeV/c
Beam intensity = $3x10^7$/spill with 1 spill/60 sec and
polarization $P_b = 0.5$
Geometrical efficiency for π^o detection = 0.25
Liquid H_2 target 100 cm long for A_N measurements
Propanediol polarized proton target 15 cm long with
polarization $P_t = 0.8$ for A_{LL} measurements.

The invariant cross section was calculated with the parameterization of Büsser et al.[17)]

$$f = E\ \frac{d^3\sigma}{d^3p} = C\ p_T^{-n}\ e^{-b\ X_T} \tag{5}$$

where $C = 14.2x10^{-27}$ cm^2/GeV^2, n = 8.6, and b = 12.5. The results are given in Table 2 for an integrated beam intensity of $1.6x10^{12}$ polarized protons corresponding to 1000 running time.

Statistical Errors

For a transversely polarized the observed single-spin asymmetry is given by

$$\varepsilon = \frac{(N_R + N_{Rb}) - (N_L + N_{Lb})}{(N_R + N_{Rb}) + (N_L + N_{Lb})} \simeq \frac{N_R - N_L}{N_{total}}$$

where $N_R(N_L)$ is the right (left) signal and $N_{Rb}(N_{Lb})$ is the right (left) background with $N_{Rb} \simeq N_{Lb}$. Then the observed asymmetry is related to

A_N through

$$\varepsilon = \frac{N_R + N_L}{N_{total}} \cdot \frac{N_R - N_L}{N_R + N_L} = \frac{1}{\chi} P_b A_N$$

where $\chi = (N_{total})/(N_R + N_L)$. The statistical error in A_N may then be approximated

$$\Delta A_N \simeq \frac{\chi}{P_b} \Delta\varepsilon$$

where $\Delta\varepsilon \simeq 1/\sqrt{(N_{total})}$. In this case the backgrounds N_{Rb} and N_{Lb} result largely from pairs of uncorrelated γ's which fall within the π^o acceptance criteria. This background can be estimated from the 2γ effective-mass distributions. With $\chi = 1.1$ as a reasonable estimate we obtain the errors ΔA_N given in Table 2.

A similar estimate has been made for ΔA_N in direct-γ production. In this case it was assumed that the ratio γ/π^o varied from 0.08 at $p_T = 3$ GeV/c to 0.2 at $p_T = 5$ GeV/c[10]. The backgrounds N_{Rb} and N_{Lb} result from the sources discussed in Sec. IIId where procedures for estimating their contributions are described. With the assumption $\chi \simeq 1.1$ we obtain the estimated statistical errors given in Table 2.

The double-spin asymmetry measurements require both polarized beam and target. The statistical error may be approximated

$$\Delta A_{LL} \simeq \frac{\chi\,\alpha}{P_b P_t} \Delta\varepsilon$$

here the 'polarization dilution factor' α reflects production on unpolarized target constituents, principally carbon and oxygen. This factor depends not only on the target material but also on the kinematic conditions, particularly p_T. To estimate ΔA_{LL} we assumed that α varies monotonically from 10-20 as p_T increases from 2-5 GeV/c. Accurate evaluation of α requires a detailed study of the A-dependence of the reaction through the relevant kinematic region.* With the assumption that $\chi \simeq 1.5$ for the double-spin asymmetry we obtain the errors ΔA_{LL} given in Table 2.

---

*It should be noted that the effect of the dilution factor is frequently overestimated. The statistical error in the asymmetry depends, in fact, only on $\sqrt{\alpha}$ since the error in the asymmetry $\Delta\varepsilon \simeq 1/\sqrt{N_{total}} \simeq 1/\sqrt{\chi\alpha(N_R + N_L)}$.

Systematic Errors

The systematic errors divide roughly into multiplicative and additive. Uncertainties in target and beam polarizations are multiplicative errors. Target polarization can be measured to ±3% with the principal uncertainty in calibration of the nuclear magnetic resonance system which uses the thermal equilibrium signal. It is estimated that beam polarization can be calculated to ±3% from the beam optics. Neverltheless, we propose to measure this independently with a high-rate polarimeter based on elastic scattering in the Coulomb-nuclear interference region[18]; this will provide an accuracy of ±5% even for runs as short as a few hours.

An additional multiplicative error in ΔA_{LL} arises from the uncertainty in target dilution α. This can be estimated with good accuracy from measurements of single- and double-spin asymmetries using liquid H_2 and a polarized proton target with identical detector conditions.

Additive errors which may introduce a spurious asymmetry in the data can arise from

i) changes in beam geometry with reversal of beam polarization

ii) misalignment of detector components

iii) changes in gain of spectrometer elements.

Geometric sources of error associated with either the beam or detector can be accurately controlled through frequent cross-checks of counting rates with different spin-spin and spin-detector (right or left) combinations. The gain stability of the Pb-glass counters will be controlled to an accuracy better than 1%. With frequent reversals of beam polarization long-term variations in gain will average away.

Comparison with Theory

The statistical errors estimated in Table 2 have been superimposed on relevant theoretical predictions in Fig. 5 and 6. Fig. 5 shows ΔA_N for π^o and direct-γ production; the QCD prediction is near zero for each. We show also the experimental results for π^o production at 24 GeV/c[6]. The greatly improved accuracy even at much larger p_T expected in the present experiment results directly from the use of a polarized beam and liquid H_2 target rather than an unpolarized beam and a polarized proton target with its large dilution factor. Up to 5 GeV/c, where QCD predictions become meaningful, asymmetries larger than 5% in inclusive π^o production and larger than 15% in direct-γ production will be reliably detected. It may be noted that the integrated luminosity ($\simeq 5\times10^{37}/cm^2$)

is comparable to that of the most extensive ISR experiments so that our measurements of cross sections for direct-γ production on H_2 will provide important new data at these energies.

Fig. 6 shows ΔA_{LL} superimposed on relavant predictions for inclusive π^o production. A significant asymmetry in the region $p_T < 3$ GeV/c would provide strong evidence against a scalar gluon for which no asymmetry is expected. Consequently, this experiment will not only discriminate among different models but it may also provide important insight into the gluon spin structure.

The double-spin asymmetry in direct-γ production cannot yet be measured with useful accuracy because of the large dilution factor α in available polarized targets. However, we place high priority on this part of the program when improved target materials reach practical use.

V. RUN PLAN AND BEAM REQUIREMENTS

As discussed earlier, the design of the gamma spectrometers has profited greatly from the long experience of the GAMS group. In addition, members of our Collaboration are currently involved in an experiment at Serpukhov which utilizes a gamma spectrometer with 500 elements identical to those proposed here; 250 have already been fabricated and are in use. These elements will become available and form the major part of the gamma spectrometers; the entire detector could be completed for early measurements in the polarized proton beam facility at Fermilab.

Before the start of data-taking with a liquid H_2 target we request 200 hours of unpolarized proton beam for checking out the entire system. A portion of this time would be run at high intensity, 6×10^8 p/spill, in order to measure the cross sections for inclusive π^o and direct-γ production with good precision. This preliminary run will provide a precise calibration of the apparatus for the purpose of detecting direct-γ's with high efficiency.

Single-spin asymmetries for both reactions will be measured simultaneously. To achieve this we request 1200 hours of polarized proton beam; this includes 200 hours for measurement of backgrounds induced by neutral hadrons. In addition, we request 1200 hours of polarized proton beam to measure the double-spin asymmetry in inclusive π^o production with the same detector conditions and the liquid H_2 target replaced by a polarized proton target.

The total request is thus:

200 hours of unpolarized proton beam, and

2400 hours ($\simeq$ 3 months) of polarized proton beam.

Because our detector is particularly compact and simple it should be compatible with detectors designed for other measurements in the polarized proton beam facility. In this case all or part of the time requested can be used simultaneously for additional measurements.

A measurement of the double-spin asymmetry in direct-γ production represents a natural extension of this program. This requires improved target materials such a LiD or NH_3 and possibly an elaboration of the detector to complete the 2π azimuthal geometry. If the new target material is available at run time this measurement will be carried out simultaneously with the measurement of A_{LL} in inclusive π^o production without the need for additional beam time.

REFERENCES

1) M.J. Alguard et al.,Phys.Rev. Lett. 37 1258,1261(1976)and 41 70(1976).
2) V.W.Hughes,Talk given at the InternationalSymposium on High Energy Physics with Polarized Beam and Targts,Lausanne, Switzerland,25 sep - 1 oct 1980.
3) J.Babcock,E.Monsay and D.Sivers,Phys.Rev.Lett.40 1161(1978) and Phys.Rev. D19 1483(1979)
4) J.Ranft and G.Ranft,Phys.Lett.77B 309(1978)
5) H.Cheng and E.Fischback,Phys.Rev. D19 860(1979)
6) J.Antille et al.,Phys. Lett. 94B 523(1980)
7) ANL-LAPP-LBL-RICE-TRIESTE Collaboration Fermilab proposal N°581
8) M.Diakonou et al.,Preprint CERN-EP/80-02 15 Jan.1980
9) A.L.S.Angelis et al.,Preprint CERN-EP/80-68 19 May 1980
10) B.Cox,Proc. 1979 International Symposium on Lepton and Photon Interactions at High Energies,Fermilab,Batavia,p602
11) D.Sivers,S.Brodsky and R.Blankenbeckler,Physics Reports 23C 1 (1976)
12) K.Hidaka,Preprint Westfield College,1980 and Proc. of the XV th Rencontre de Moriond,Savoie,France,March 1980
13) IHEP-IISN-LAPP Collaboration, SPS proposal, SPSC/P110
14) G.A.Akopdjanov et al.,Nuc.Instr.&Method 140 441 (1977)
15) V.A.Davidov et al., Nuc. Instr. Methods 145 267(1977)
16) T.Kusumegi,Private communication
17) F.W.Büsser et al.,Nuc.Phys. B106 1(1976)
18) K.Kuroda A.Penzo and V.Soloviancv,EP internal report 79-1 Jan.1979
19) V. Bouffard et al. to be published in Journal de Physique.

TABLE 1

Parameters and characteristics	
- Lead-glass cell dimensions	38×38×450 mm^3
- Type of glass	F-8
- Total number of cells	744
- Working area and weight of the spectrometer	0.8 m^2, 2.5 t
- Photomultiplier	FEU-84-3
- Accuracy in measuring photon coordinate	
at 25 GeV	± 2 mm
at 200 GeV	± 1 mm
- Photon energy resolution	
at 25 GeV	± 2.5 %
at 200 GeV	± 1.5 %
- Mass resolution for decaying particles	a few %
- Time resolution	40 nsec gate

TABLE 2

p_T (GeV/c)	X_T	ΔX_F	Δp_T	n	ΔA_N %	n	α	ΔA_{LL} %
2	0.17	0.1	0.5	———	———	4.4×10^6	10	± 0.39
3	0.25	0.125	1.0	7.8×10^5	±0.22	1.2×10^5	13	± 2.8
4	0.34	0.15	1.0	2.8×10^4	±1.3	4.1×10^3	17	±16.9
5	0.42	0.20	1.0	1.9×10^3	±4.8	2.8×10^2	20	±69.0
6	0.51	0.30	1.0	2.1×10^2	±14.0	3.1×10^1	—	———

TABLE 3

p_T (GeV/c)	X_T	ΔX_F	Δp_T	γ/π°	n	ΔA_N %
3	0.25	0.125	1.0	0.08	6.3×10^4	±1.0
4	0.34	0.15	1.0	0.12	3.3×10^3	±4.4
5	0.42	0.20	1.0	0.15	2.9×10^2	±14.5
6	0.51	0.30	1.0	0.19	3.9×10^1	±39.0

For the reason of simplicity we present here $p_\perp$ corresponding to the average cross section of the (non-symmetric) binning. The weighted p_T is about 0.15 GeV/c less than the indicated one but the correction to be introduced in the cross section is less than the ambiguity on the experimental values at large $p_\perp$ region.

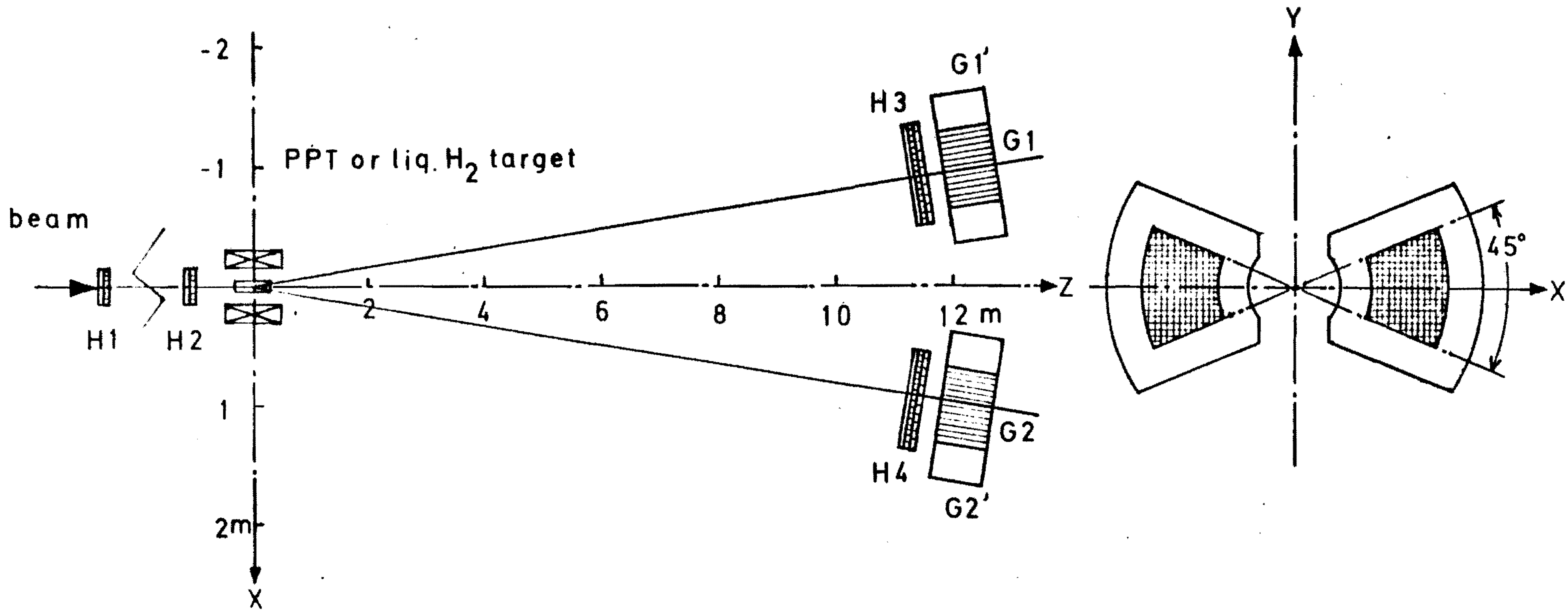

-2
-1
PPT or liq. H_2 target
beam
H1
H2
1
2m
X
2
4
6
8
10
12 m
Z
H3
G1'
G1
H4
G2
G2'
Y
X
45°

Fig.1

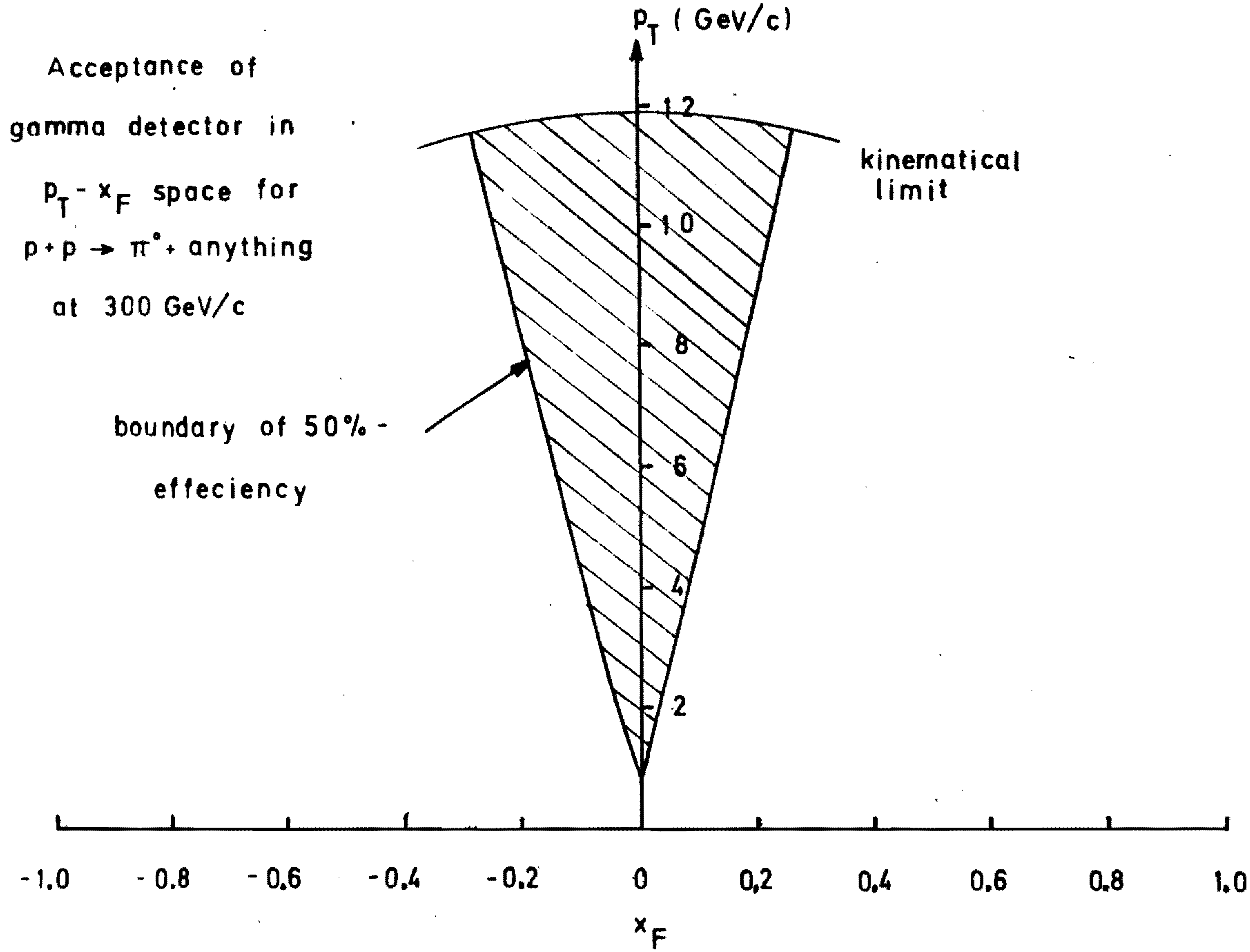
Acceptance of
gamma detector in
$p_T - x_F$ space for
$p + p \rightarrow \pi^\circ +$ anything
at 300 GeV/c
p_T (GeV/c)
12
10
8
6
4
2
kinematical
limit
boundary of 50% -
effeciency
-1.0
- 0.8
- 0.6
- 0.4
- 0.2
0
0.2
0.4
0.6
0.8
1.0
x_F

Fig. 2

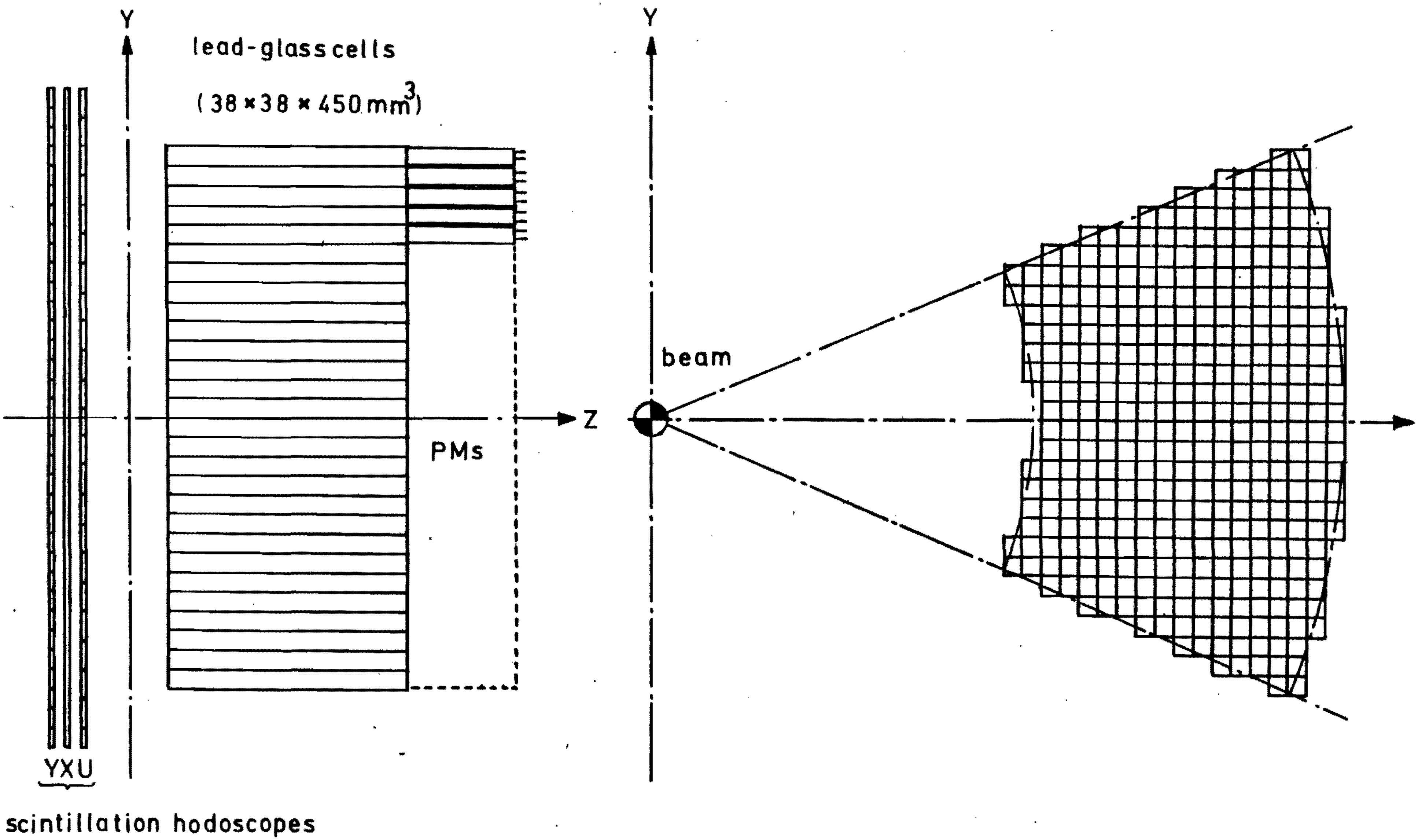
Y
lead-glass cells
(38 × 38 × 450 mm³)
Z
PMs
YXU
scintillation hodoscopes
Y
beam
X

Fig. 3

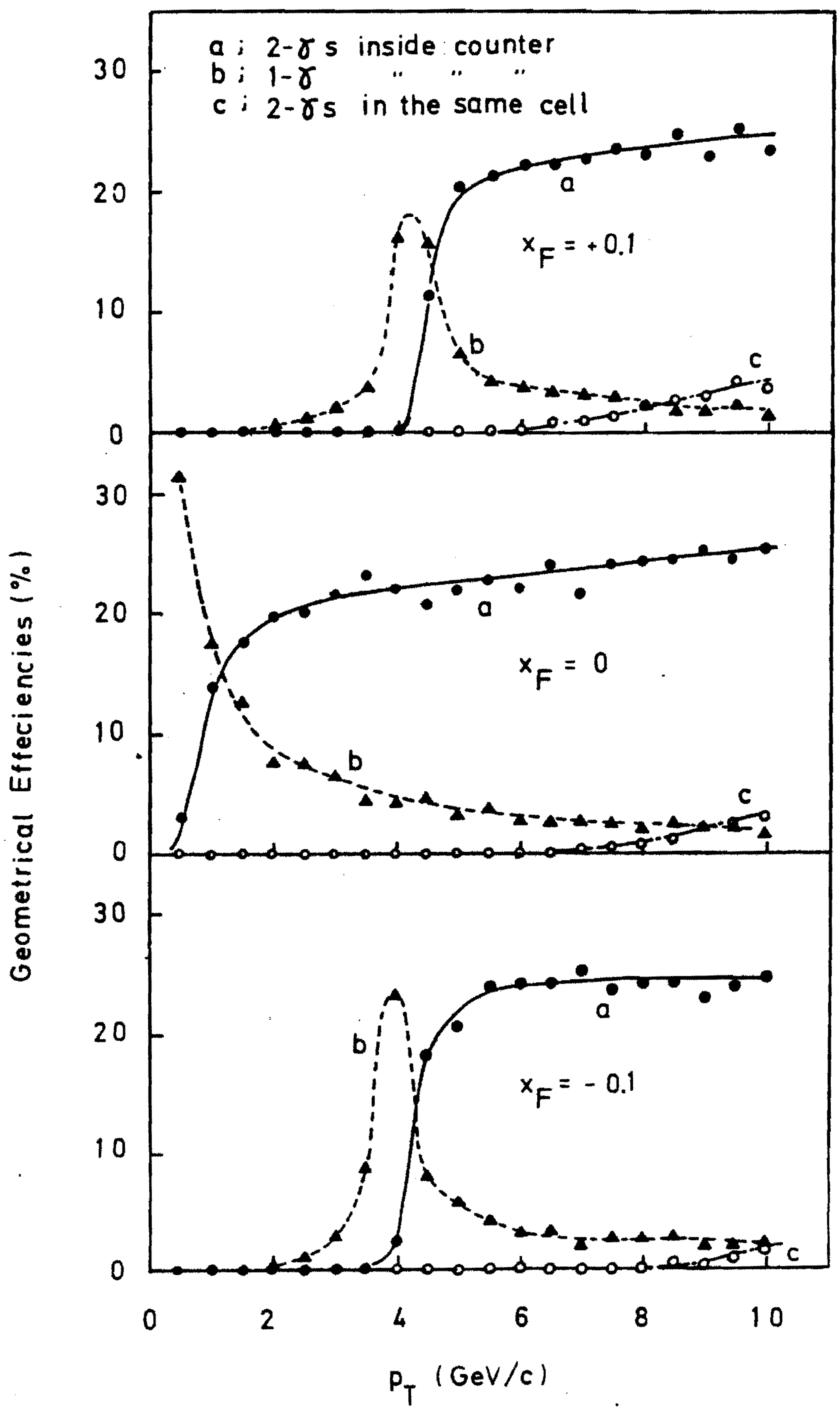
a ; 2-γ s inside counter
b ; 1-γ " " "
c ; 2-γ s in the same cell
x_F = + 0.1
x_F = 0
x_F = - 0.1
a
b
c
Geometrical Effeciencies (%)
0
10
20
30
0
2
4
6
8
10
p_T (GeV/c)

Fig. 4

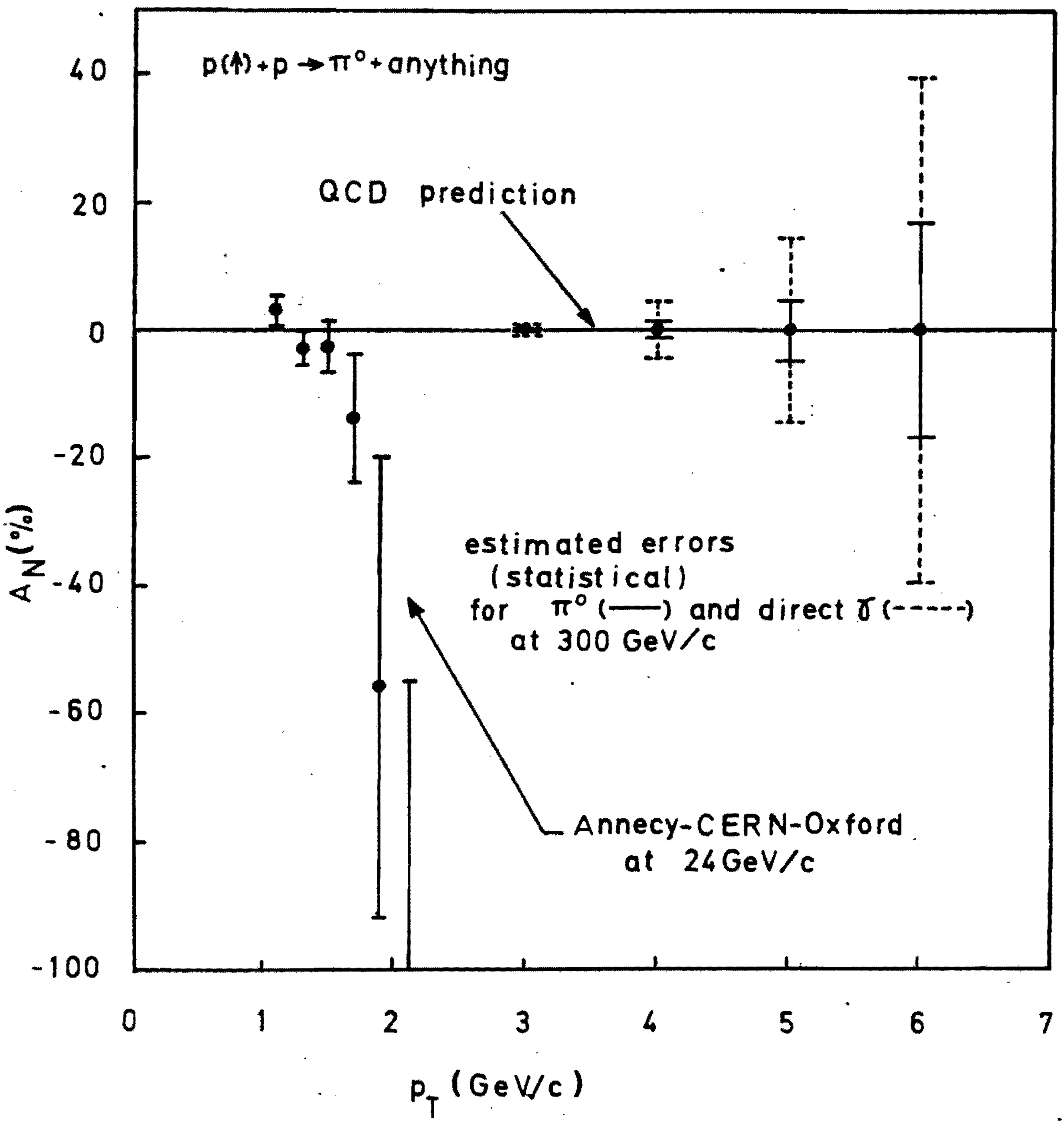
p(↑)+p → π° + anything
QCD prediction
estimated errors
(statistical)
for π° (——) and direct γ (-----)
at 300 GeV/c
Annecy-CERN-Oxford
at 24GeV/c
A_N(%)
40
20
0
-20
-40
-60
-80
-100
0
1
2
3
4
5
6
7
p_T (GeV/c)

Fig. 5

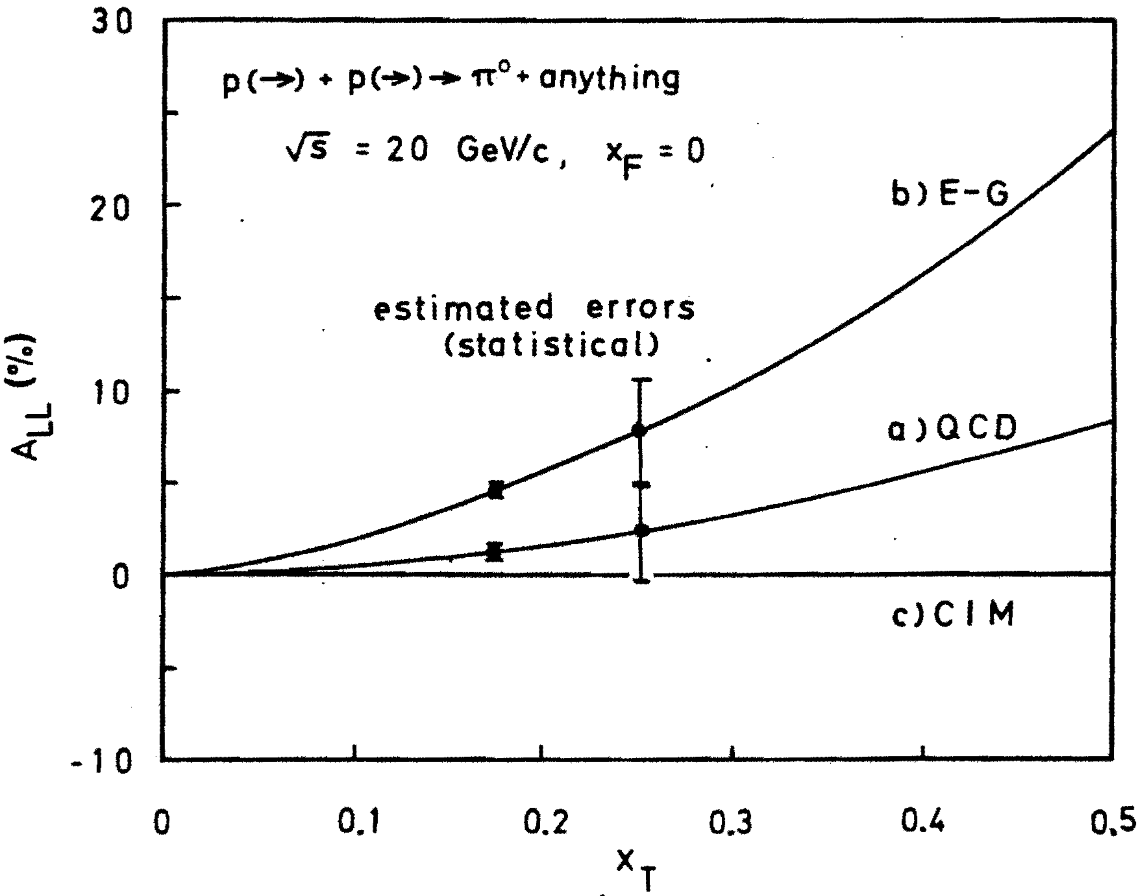

30
20
10
0
-10
0
0.1
0.2
0.3
0.4
0.5
x_T
A_{LL} (%)
p(→) + p(→) → π° + anything
√s = 20 GeV/c, x_F = 0
b) E-G
a) QCD
c) CIM
estimated errors
(statistical)

Fig. 6

678 Addendum

INSTITUTE FOR HIGH ENERGY PHYSICS

V.D.Apokin, A.N.Vasiliev, A.A.Derevschikov, Yu.A.Matulenko,
A.P.Meshcnin, S.B.Nurushev, L.F.Soloviev, V.L.Solovianov

STUDY OF SPIN EFFECTS IN INCLUSIVE PRODUCTION OF PIONS AND PROMPT PHOTONS AT LARGE MOMENTUM TRANSFER ON FNAL TEVATRON POLARIZED BEAM

Serpukhov, 1981

INTRODUCTION

A series of experimental investigations carried out at the IHEP U-70 accelerator during 1973-76 made it clear that polarization effects in elastic hadron collisions do not vanosh with energy growth/1-3/ as it was expected from the predictions of the most of theoretical models. Later on similar results were obtained at CERN/4/ and Fermilab/5-7/. Moreover the investigation of spin effects in inclusive reactions, e.g. in Λ /8-11/ and π^o meson/12/ production revealed a large value for Λ particle polarization (30%) and asymmetry in π^o meson production on a polarized target (~ 50%). Nowadays there is not a single model that would be able to give a quantitative description of the effects mentioned above. Hence further development of theoretical models is to be undertaken together with accumulation of experimental data on porarization phenomenon in high energy hadronic physics.

A unique polarized proton beam to be constructed at the Tevatron Lab/13/ will provide all the conditions required for the experiments on polarization in the earlier unattainable energy range, thus giving us a possibility to investigate the role of constituents in transferring the information about the spin in interactions at TeV energies.

This proposal suggests to carry out a systematic study of asymmetry in inclusive pion production in the following reactions:

1. A polarized beam + unpolarized target

$$p_{\uparrow} + A \rightarrow \pi^{+,0,-} + X . \qquad (1.1)$$

Here A stands for the set of nuclear targets. In this reaction the dependence of the so-called single-spin asymmetry on atomic weight of a nucleus is being studied.

2. A polarized beam + a Polarized target

$$p_{\uparrow} + p_{\uparrow} \rightarrow \pi^{+,0,-} + X \qquad (1.2)$$

The so-called spin-spin asymmetry, determining corelation between spin orientation and pion production inclusive cross section is studied in this reaction.

At the incident momentum of 500 GeV/c the apparatus, offered below, allow one to investigate the asymmetry effects within the range of kinematical parameters $-0.2 \leq x \leq 0.3$, $0.5 \doteq p_T < 5$ GeV/c.

II. PHYSICAL MOTIVATION

At present the only real candidate for the theory of strong interaction is quantum chromodynamics (QCD). Application of QCD in the framework of perturbation theory for descroption of hadron production at large momentum transfer turned out to be quite promising. However the calculations made it clear that to destinguish the QCD prediction from those of other models one should carry out measurements of single-particle inclusive cross sections at $\sqrt{s} \geqslant 200$ GeV, which cannot be achieved at modern accelerators. At the sametime QCD is known to be a gauge-invariant theory of interaction of a color triplet for quarks with 1/2 spin and color octet of gluons with 1 spin. Therefore one may suppose that within the framework of this theory an essential role in interaction dynamics is played by spin effects. As it became clear from relevant calculations[14-17], quite noticeable spin-spin effects are observed in fundamental processes ($qq \to qq$, $q\bar{q} \to q\bar{q}$, $\bar{q}\bar{q} \to \bar{q}\bar{q}$, $qv \to qv$, $\bar{q}v \to \bar{q}v$, $q\bar{q} \to vv$, $vv \to q\bar{q}$ and $vv \to vv$). Together with assumption that quarks and gluons "remember" the spin of their parental proton, these effects may results in a considerable asymmetry in inclusive hadron, pions in particular, production at large momentum transfer

$$A_{ik} = \frac{d\sigma[p(i)p(k) \to \pi X] - d\sigma[p(i)p(-k) \to \pi X]}{d\sigma[p(i)p(k) \to \pi X] + d\sigma[p(i)p(-k) \to \pi X]}, \quad (II.1)$$

where i, k designate the direction of incident proton polarization. The quantity A_{ik} is rather sensitive for the spin distribution functions of quarks and gluons on nucleons.

In a particular case, when one of incident protons is polarized, QCD predicts a zero-spin asymmetry A[18]. In the case when both incident protons have polarizations perpendicular to their momenta, spin spin asymmetry effect turns out to be rather small. And only in the case when both initial spins are parallel to the beam direction, one may expect large asymmetry effects[14]. It is equivalent to the statement that quarks and gluons cannot carry information about transverse polarizations in strong interactions.

Fig. 1 presents the value for asymmetry A_{LL} versus $X_\perp = 2P_T/\sqrt{S}$ calculated according to QCD for inclusive pion production[14]. Three types of distribution have been considered for the constituents. As is seen the largest asymmetry effect is expected in the case of Carlitz-Kaur distribution and may make up almost 10% at $x = 0.4$. In this model the largest contribution to the quantity A_{LL} is made by the elementary $qq \to qq$ reaction at large $x_\perp$ ($x_\perp \geq 0.7$), at small and moderate $x_\perp$ the contribution from the subprocesses $qv \to q$ becomes significant, and at small $x_\perp$ it is the contribution from processes $qv \to v$, $vv \to v$ which is of importance (here v gluons). At the same $x_\perp$ asymmetry is 3% and 6% in two other models, respectively. A value of asymmetry A_{LL} in inclusive π^+ and π^- meson production (see fig. 1b) is a factor very sensitive to helicity transfer by different constituents. As is seen from the figure, in the di-quark model, where all the information about spin orientation is carried by the leading u-quark, $\Delta d(x)=0$ (Δ define the capability to carry spin information) and for inclusive π^- meson production $A_{LL}=0$ (in reality A_{LL} is not exactly equal to zero due to contribution from the uu → uu process, which is suppressed quite noticeably). The sign of A_{LL} is negative for π^- meson production in two other distributions (conservative SU(6) distribution and Carlitz-Kaur distibution) since the value for $\Delta d(x)$ is negative. The relative value for asymmetry A_{LL} for π^- meson with respect to π^+ meson characterises a relative capability of d-quarks to carry spin with respect to u-quarks. For the conservative SU)6) model $A_{LL}(\pi^-)/A_{LL}(\pi^+)\leq 0.4$, while in the Karlitz-Kaur model $A_{LL}(\pi^-)/A_{LL}(\pi^+)\leq 0.1$. This means that in the Karlitz-Kaur model d-quarks have quite less capability to carry spin information, than in the conservative SU(6) model.

From the same figures it is seen that the measurement of asymmetry with an accuracy of some percent within the interval up to x = 0.4 allows one to distinguish between these two models.

In calculations made in the framework of QCD with application theory single spin asymmetry turns into zero in the first (pole or Born) approximation and this assertion was used in earlier calculations. Therefore it is very desirable to obtain experimental confirmation of these predictions. Moreover from recent experiments[8-11] it became clear that in inclusive reactions with Λ particle production the latter ones is polarized, quite considerably (see fig. 2). At lower energies (24 GeV) a noticeable asymmetry was observed in inclusive π^0 meson production in the central region at large momentum transfers/12/ (see fig. 3). It might also be that both Λ and π^0 mesons were mainly produced from the decays of other resonance states, arising from interaction of constituents (quark, gluons). Clarification of this questions needs further experimental and theoretical studies.

This proposal suggests to measure asymmetry in reactions (1) and (2) within the range of $-0.2 \leq x \leq 0.2$, and $1 \leq p_T < 5$ GeV/c on a polarized proton beam of FNAL Tevatron. This results will be obtained simultaneously for all kinds of pions and they will allow to distinguish the aforementioned theoretical models. If necessary the same apparatus may be used in investigation of assymmetry in resonance production of vector mesons as well as of hyperons .

III. POLARIZED BEAM OF FNAL TEVATRON

The layot of the beam channel units used to form and transport a polarized proton beam in presented in fig. 4. A possibility to create a transversaly polarized beam as well as a longitidinally polarized one in a wide energy range, Tevatron energy including, has been forseen in this beam channel. A symmetric triplet scheme is used to form a polarized proton beam from Λ decay. An intermediate focusing point where a correlation between the beam position and its polarization (spin dispersion) exists is forseen. This will be used for "tagging" of polarization. Eight magnets are to be installed at the end of the beam channel ("snake") for polarization reverse in each cycle without any displacement of the beam direction. Each magnet has a magnetic field integral of 2.74 Tm. The experimental equipment to be installed after the target will occupy about 3.0m.

Next figure (fig. 5a) illustrates the scheme for neutral beam-dump and particle selection by their momentum (beam acceptance is ± 5%). The optical scheme of the beam with the intermediate and end focus is shown in fig. 5b. The expected intensities of the proton and antiproton beams with 45% polarization are given in fig. 6 for the case when the beams are formed in the modern 400 GeV accelerator as well as in the 1000 GeV Tevatron. As is seen from the figure, the Tevatron may provide a polarized proton beam with the momentum of 500 GeV/c and intensity of $3\cdot10^7$ polarized proton per cycle. At point of the locations of an experimental target the beam dimensions are $\rho \leq 20$ mm, and divergencies in both planes are ± 1 mrad which completely satisfies the requirements imposed on the beam characteristics.

Though the average polarization of the beam can be calculated with a sufficient accuracy (± 3%) still it should be investigated experimentally and be monitored at different polarization. It should also be compared with a nonpolarized beam. For this purpose a polarization effect is planned to be used which arises due to the interaction of proton magnetic moment with nucleus Coulomb field[19,20]. Fig. 7 illustrates the expected effect caused by such an electromagnetic interaction (P_{em}), by strong interaction (P'_N) and the summed polarization effect (P_{Tot}) versus t.

To measure the polarization we plan to use the devices shown in fig. 8a alongside with the processor (fig. 8b)[22]. Hodoscopes H1-H3 provide preliminary angular selection of particles, while a more precise analysis both of the angle and momentum of scattered particles is performed by proportional chambers

PC1-PC6. For an "active" target we propose to use a set of thin scintillation counters, which detect recoil protons and measure their energy. From preliminary tests it has become clear that such a combination of devices allows a better selection of elastic scattering[23].

We estimated the time necessary to measure polarization in Coulomb-nuclear interference. It was done under conditions that:

- detector-scintillation target, 10 counters each 2 mm thin (0.15 g/cm^2 hydrogen);
- incident momentum 500 GeV/c;
- polarized beam intensity $2 \cdot 10^7$ ppc (cycle duration is 20 s)
- signal/background ratio 1;
- $\Delta\varphi/2\pi$ (acceptance in azimuthal) $\simeq 1$;
- the events are integrated within the interval $2\ 10^{-2} \leq |t| \leq 2\ 10^{-1}$ $(GeV/c)^2$;
- the accuracy in measuring the asymmetry is $\Delta\mathcal{E} = 2\ 10^{-3}$
- satefy factor for the experiment is 2.

Thus in accordance with what was said above 2 days are needed for statistics aqcuisition. The Table 1 below gives the parameters of the detectors used for a polarized beam calibration.

IV EXPERIMENTAL SETUP

The experimental set-up for simultaneous detection of charged and neutral pions emitted from the target after bombardment by a polarized beam is presented in fig. 9. Two units of gamma-detectors LGD and RGD, consisting of 500 counters each and installed symmetrical with respect to the beam axis are to be used for photon detection. In creation of these devices the ideas of work[24] were of great help for us. Each unit is installed in such a way that the angular interval of $65^\circ - 115^\circ$ is observed in the c.m.s. In the lab. system the central line runs through gamma-detector at 3.9° with respect to the beam axis and the angular acceptance is 1.7°.

Hadrons and electrons may also hit the gamma detector. The information from the proportional chambers may be used for their identification and for the definition of their momenta and the entrance points. This information is read out in the case when a "neutral trigger" N_T = beam$\cdot\overline{(S1\cdot S2)}\cdot\Sigma$(where Σ is the sum of signals from the gamma-detector) is accompanied by a signal from the SL (SR) detector. The comparison of energy released from the gamma detector with the charged particle momentum measured with the help of a magnetic spectrometer will allow to identify particles that occur in the gamma detector.

Charged pions are detected and their momenta are measured with the magnetic spectrometer consisting of proportional chambers PC1-PC4 and SCM105 magnet with the aperture of 213x51 cm^2 (width x height), and effective length of 1 m and the field B equal to 1.25 Tm. The information from the TH1-TH4 hodoscopes is used as a trigger. A trigger for charged particle is generated as follows

1. N_1= Beam$\cdot\overline{(S1\cdot S2)}$;

2. $N_2 = N_1\cdot\Sigma_1\Sigma_2\cdot\Sigma_4$ where Σ_i is the sum of signals of i-th hodoscope;

3. $N_{14}(Y) = Y_1(i)Y_4(K)$ with the help of a special matrix $\theta_{1Y}(Y)$ with 9 x 30 inputs (which corresponds to the number of elements in the Y-th plane TH1 and TH4) particles emitted from the target are selected. In this we use the fact that in the vertical plane the magnetic field does not act on the particle and the event is presented with a straight line.

4. $N_{12}(X) = X_1(i)X_2(K)$;

fixed angles θ_x are selected with a special matrix $\theta_{12}(x)$ with 10 x 22 inputs (which corresponds to the number of elements in the x-th plane TH1, TH2);

5. Cut-off in the transverse momentum P_{TX} = 0.7 GeV/c; This requirement leads to the dependence $P_c(\theta_x)=\frac{0.7}{\theta_x}$ where $P_c(\theta_x)$ is the boundary momentum (see fig. 10a). The events with momenta $P \geqslant P_c(\theta_x)$ are the ones useful for us. This condition results in the correlation θ_x particle production angle and its position in the hodoscope TH4 (fig. 10c). A special matrix P_x will be used to extract a useful area, dashed in the figure.

According to the estimates the cut-off $P_{TX}=0.7$ should suppress the trigger 5-10 times. Consequently the final trigger is formed in the following way $T = N_2 \cdot N_{14}(Y) \cdot P_x$ (IV.1).

As one can understand from what was said above we proceed from the fact that in the vertical plane any event is presented with a straight line and at a fixed angle a given cut-off over P_{TX} (a horizontal component of a transverse momentum) defines the range of useful particle momenta.

However the measure asymmetry effect may be distored by a contribution from other particles, which can be seen from the relation

$$\varepsilon_e = \alpha_\pi \varepsilon_\pi + \alpha_K \varepsilon_K + \alpha_p \varepsilon_p , \qquad (IV.2)$$

where α_π, α_K, α_p are pion, kaon and proton fraction in the number of detected events, ε_e the measured asymmetry effect, ε_π ε_K, ε_p are effects caused by pions, kaons and protons respectively. We assume that the spectrometer differentiate particles by charge so that, ε_e is defined individually for negative and positive particles. From the data of work[25] at $\sqrt{S}$ = 31 GeV and for p_T = 0,28 GeV/c we find α_{π^+} = 88,3%, α_{K^+} = = 6,5%, α_p = 5,2%, α_{π^-} = 87,5%, α_{K^-} = 10%, $\alpha_{\bar{p}}$ = 2,5%. For an approximate estimate we shall assume that, ε_π = 1%, $\varepsilon_K = \varepsilon_p$ = = 10% and from the quoted relation it is seen that the contribution from the background terms is identical to the one from the required reaction. Consequently, the contribution from background particles should be suppressed at least ten times, in order the required symmetry be not distorted by 10%. Two threshold multichannel Cerenkov counters Č1 and Č2 are planned to be used for this purpose. These counters cover the whole momentum interval we are interested in and allow one to suppress K-meson and proton detection. The number of photoelectrons produced on the photocathode of the Cerenkov counter photomultiplier is equal to

$$N = KL \sin^2\theta \quad , \tag{IV.3}$$

where K is the factor 100 for good light-collection and high cathode quantum efficiency L is the counter lenght in cm, is Cerenkov radiation emission angle. This is defined through the reflection factor n

$$\sin^2 = 1 - \frac{1}{n^2\beta} \simeq \Delta n - \frac{m^2}{p^2} \; , \tag{IV.4}$$

where $\Delta n = n^2 - 1$, m and p are particle mass and momentum. The threshold of one of the counters will be defined from the conditio

$$\Delta n = \frac{m_K^2}{p^2} = 2{,}44 \; 10^{-5} \tag{IV.5}$$

The threshold of the second counter is to be at intermediate energies, which can be found from the condition for equality of minimal efficiencies

$$\frac{m^2}{p^2_{min}} - \frac{m^2}{p^2_{\pi}} = \frac{M^2}{p^2_{\pi}} = \frac{M^2}{p^2_{max}}$$

Whereof

$$p_{\pi} = 35 \text{ GeV/c} \; , \tag{IV.6}$$

Then the minimal number of photoelectron is equal to N_{min} 2 f.e. and the counter efficiency is

$$\varepsilon_{min} = 0.86 \; . \tag{IV.7}$$

The conclusion is at least two threshold mulctichannel Cerenkov counters are necessary to suppress the background events. The main parameters of the devices described above are enlisted in the Table 2.

Calibration of the gamma-detector requires electron beam with momentum of 100 GeV/c. For the tuning of all the other devices we need a test beam of relativistic particles.

V. ESTIMATES OF TIME CONSUMPTION

To estimate the rate of Data taking we shall adopt the following initial conditions:

- polarized proton beam intensity per cycle $I_0 = 2\ 10^7$;
- polarization of the beam P = 0,45 beam energy, E = 500 GeV - number of cycles per hour N = 60;
- momentum transfer interval p = ± 0,5 GeV/c - X variable interval $\Delta X = \pm 0,2$;
- signal background ratio = 1;
- π-meson inclusive production cross section for $P_T > 1$ GeV/c $\sigma_{inv} = \sigma_1 \cdot p^{-8}$, where $\sigma_1 = 1,6\ 10^{-27}$ cm^2
- the target is of two types: either 100 cm liquid hydrogen one or a polarized ^{6}LiD, 15 cm long. The dependence of the precision of asymmetry measurements versus the momentum transfer for the liquid hydrogen target is presented in fig. 11. Broken line has been calculated for a 30 day run with a polarized target, solid line for liquid hydrogen target. Since in the considered interval of x and p variations inclusive cross sections for charged pions production practically coincide, then the results will be practically in paralell obtained for them with the same precision. The set of the data obtained will allow us to carry out a qualitative check of the QCD predictions in the range of hard collisions of hadron constituents.

It is assumed that the beam chaneal has been tuned and beam polarization has been calibrated in separate runs. To start the adjustment of the devices mentioned above three runs, each one weak long are needed. With account for the reliability factor of type 1.5 the whole experiment will consume abount 3 months.

VI. PROMPT PHOTON DETECTION

If some additions are made to the described devices, the system will be able to detect not only pions but prompt production of photons, the process which attracts great interest during last year. The thing is the photons, on contrary with pions, participate in hard (high energy) collisions themselves and the main source of their production is the reaction gluon+ quark γ + quark, i.e. quantum-chromodynamic Compton effect. As it became clear from recent investigations the ratio of the prompt photons to π^0 mesons increases with the growth of P_T as it was expected from QCD. Availability of a polarized high energy proton beam garantees a more reliable selection of prompt photons, as compared with the case of a polarized target. As for the background, the main sources are:

a) decays $\pi^0, \eta^0 \to 2\gamma$ where one of the photons misses the detector (or it has small energy) or both photons merge (they cannot geometrically be distinguished);

b) neutral hadrons, e.g. n, $\bar{n}$, K^0_L etc producting showers.

To reduce the contribution from these processes to prompt-production of photons we plan to surround the units of the gamma detector with guard counters (see fig. 12). From Monte-Carlo calculations it became clear that with the width of counters of about 30 cm we shall be able to suppress about 97% of events from the quoted background processes in the range of $x \simeq 0$ and $P_T \simeq 56$ GeV/c. To distinguish between the contributions of the showers from neutral hadrons and photons lead plates of $\simeq 10\ X_0$ thick may be installed between corresponding hodoscopes and gamma-detector units. In this case the showers in the gamma-detectors are produced mainly by hadrons and having introduced a correction for absorption of these hadrons in the lead plates one may define their total contribution to the detected events. Depending on the values for x and p_T this contribution should vary within 10-40% as it was demonstrated by the experiments at FNAL.

Under the same requirement what were adopted in the estimates of the statistics for pions, we find the expected measument accuracy for one-spin asymmetry in inclusive production of prompt photons (see fig. 13). As is known in QCD this quantity is equal to zero and any value different from zero, may make QCD predictions rather doubtful.

On the part of the Institute for High Energy Physics we may contribute two units of gamma-detectors, 500 channels in each and two Čerenkov threshold counters Č1 and Č2.

R E F E R E N C E S

1. C.Bruneton, J.Bystricky, G.Cozzika et al., Phys.Lett., 44B, 471, 1973.
2. A.Gaidot, C.Bruneton , G.Cozzika et al., Phys.Lett. 57B, 389, 1975
3. К.Брюнетон, И.Быстрицки, А.Гедо и др. ЯФ 25,369,1977; Phys.Lett., 61B, 103, 1976.
4. G.Fidecaro, M.Fidecaro, L.Lanceri et al., Phys.Lett. 76B,369,1978; Nucl.Phys. B173, 513, 1980.
5. J.H.Snyder ,A.Yokosawa et al. Phys.Rev.Lett., 41, 781, 1978.
6. M.D.Corcoran. Phys.Rev.Lett., 40, 1113, 1978.
7. R.V.Kline, I.P.Auer, W.Brücker et al. Phys.Rev., 22D, 553, 1980.
8. G.Bunce, K.Heller, O.Overseth et al. Phys.Rev.Lett., 36, 1113,1976
9. K.Heller, G.Bunce, O.Overseth et al.,Phys.Lett., 68B, 480, 1977.
10. K.Heller, G.Bunce, O.Overseth et al. Phys.Rev.Lett.,41, 607, 197
11. S.Erhan et al. Phys.Lett., 82B, 301, 1979.
12. J.Antille, L.Dick, K.Kuroda et al.
13. I.P.Auer, E.Colton, H.Halpern. Construction of polarized beams and an enriched antiproton beam facility in the meson laboratory and experiments using such a facility. Fermilab Proposal № 581, January 27, 1978.
14. J.Babcock, E.Monsay and D.Sivers. Phys.Rev., 19, 1483, 1979.
15. K.Hidaka, E.Monsay and D.Sivers. Phys.Rev., 19, 1503, 1979.
16. J.Ranft and G.Ranft. Phys.Lett., 77B, 309, 1978.
17. C.K.Chen. Phys.Rev.Lett., 41, 1440, 1978.
18. G.Kane, J.Pumplin and W.Repka. Phys.Rev.Lett., 41, 168, 1978.
19. B.Z.Kopelovich and I.Lapidus. Soviet J. Nucl.Phys. 19, 218, 1974.
20. C.Bourrely, J.Soffer and D.Wray. Nucl.Phys., B77, 386, 1974.

21. A.Apokin, W.Bartl, R.Birsa et al. Study of spin effects at SPS energies using a polarized proton beam. Proposal CERN/SPSC/77-61, SPSC/p 87, July 19, 1977.

22. A.A.Derevshchikov, Yu.A.Matulenko, S.Nurushev et al. Nucl.Instr Meth. 108, 381, 1973.

23. K.Kuroda, A.Penzo, V.Solovyanov. Preprint CERN, EP Internal Report 79-1, 1-15, 17 Januar 1979.

24. Г.А.Акопджанов, А.В.Инякин, В.А.Качанов и др. Препринт ИФВЭ, ПЭФ 76-IIO, Серпухов I976; Nucl.Instr.Meth., 140, 441, 1977.

25. K.Guettler, B.G.Duff, G.Giacomelli et al. Phys.Lett., 64B, 111, 1976.

26. B.Alper, H.Boqqild, G.Jarlskog et al. Phys.Lett., 44B, 521, 1973.

27. A.L.S.Angelis, B.J.Blumenfeld, L.Camilleri et al. Phys.Lett., 79B, 505, 1978.

28. M.Banner, J.L.Hamel, J.P.Pansart et al. Phys.Lett., 44B, 537,1973.

FIGURE CAPTIONS

Fig. 1. Asymmetry A_{LL} for reactions $p_{\uparrow} + p_{\uparrow} \rightarrow (\pi^{o}$ or jet) + + X(A) and $p_{\uparrow} + p_{\uparrow} \rightarrow (\pi^{+}$ or π^{-}) + X(B) versus $x_{\perp} = 2p_{T} / \sqrt{s}$: (a) for conservative SU(6) distributions, (b) for quark distributions and (c) Carlitz-Kaur distributions.

Fig. 2. The Λ polarization as a function of p_{T} for initial momenta: 24 GeV/c /9/, 300 GeV/c /8/, 400 GeV/c /10/, 1,5 and 2,0 TeV/c /11/.

Fig. 3. The asymmetry for $p + p_{\uparrow} \rightarrow \pi^{o} + X$ as a function of p_{T} at the momentum of 24 GeV/c /12/.

Fig. 4. The overall view of the proposed polarized-beam line.

Fig. 5. Sketch of beam line (a) and beam envelopes for triplet version. The crosses (x) show the effect of $\pm$ 5% momentum bite.

Fig. 6. Predicted intensities for polarized proton and anti-proton beams with 400 and 1000GeV/c targetting.

Fig. 7. Polarization in pp elastic scattering at 500 GeV/c for small $|t|$ values.

Fig. 8. A set-up for calibration of beam polarization by measuring the asymmetry in region of Coulomb-nuclear interference (a) and (b) a block-scheme of the fast processor.

Fig. 9. Experimental set-up for the simultaneous measurements of asymmetries in the inclusive production of $\pi^{+,-,o}$ by polarized beam of Tevatron of FNAL: a) Top view b) side view.

Fig. 10. Horizontal projection of scattering angle versus a momentum p of the particle at a cut p_T = 0.7 GeV/c; a shaded region is not detectable (a). Correlation between scattering angle θ_x and a position of particle at hodoscope TH4 for a cut p_T = 0.7 GeV/c (b). The shaded region corresponds to the useful events for both charges of pions .

Fig. 11. The accuracy of asymmetry measurement in inclusive π^o -production for 30 days run; solid line - for hydrogen target, dashed line - for polarized target.

Fig. 12. Additional hodoscopes HL and HR and the gard counters G1 and G2 for a detection of prompt- gamma quants.

Fig. 13. Single-spin asymmetry A_N versus p in reaction $p + p_{\uparrow} \rightarrow \pi^o + X$ at momentum 24 GeV/c. For $p_T >$ 3 GeV/c it is shown the asymmetry in π^o and prompt-gamma production estimated for 300 GeV/c.

Table 1

Parameters of detectors to be used for measurements of the polarization in the Coulomb-nuclear interference region

	Detectors	Dimensions X x Y (mm^2)	Number of planes	Pitch (mm)	Total number of wires	Number of PM
1	PC1	50 x 50	2x, 2y	1	200	
2	PC2	50 x 50	2x, 2y	1	200	
3	PC3	50 x 50	2x, 2y	1	200	
4	PC4	100 x 100	2x, 2y	1	400	
5	PC5	500 x 500	x, y	2	500	
6	PC6	500 x 500	x, y	2	500	
7	H1	50 x 50	x, y	2	-	50
8	H2	26 x 26	x, y	2	-	26
9	H3	100 x 100	x, y	2	-	66
10	"Active" target	30 x 30	thickness 2 mm			15

Table 2

Main parameters of Gamma Detector

1. Lead-glass cell dimensions, mm^3	38x38x450
2. Type of glass	T -1-00
3. Total number of cells	1000
4. Working area, m^2	1,2
5. Weight of the spectrometer, t	5
6. Photomultiplier	FEU-84-3
7. Accuracy in measuring photon coordinate	
at 40 GeV, mm	± 2
at 200 GeV, mm	± 1
8. Photon energy resolution	
at 40 GeV, %	± 2,5
at 200 GeV,%	± 1,5
9. Mass resolution for decaying particles	± 5%
10. Time resolution, nsec	40
11. Number of acceptable events, ev/sec	500

Table 3

Main parameters of hodoscopes

1	Hodoscope	x (cm)	Δx (cm)	y (cm)	Δy (cm)	N_x	N_y	z (m)
1	TH1	30	3	9	1	10	9	1
2	TH2	132	6	42	1	22	42	6,5
3	TH4	330	12	90	3	28	30	14

Table 4

Parameters of proportional chambers

	Proportional chambers	Dimensions (XXY), cm	Pitch, mm	Number of PM X	Number of PM Y	z, m
1	PC1	35 x 10	2	175	50	0,8
2	PC2	150 x 50	2	750	250	6,3
3	PC3	200 x 50	3,2	700	250	8,3
4	PC4	400 x 110	4,2	1000	550	13,5

Table 5

Parameters of Cerenkov counters

	Entrance (XXY), cm	Exit (XXY), cm	Length m	Gas	Number of PM	E_{th}, GeV
$\check{C}_1$	40 x 15	200 x 60	4	He	20	35
$\check{C}_2$	250 x 60	450 x150	4	H_2,He	30	10

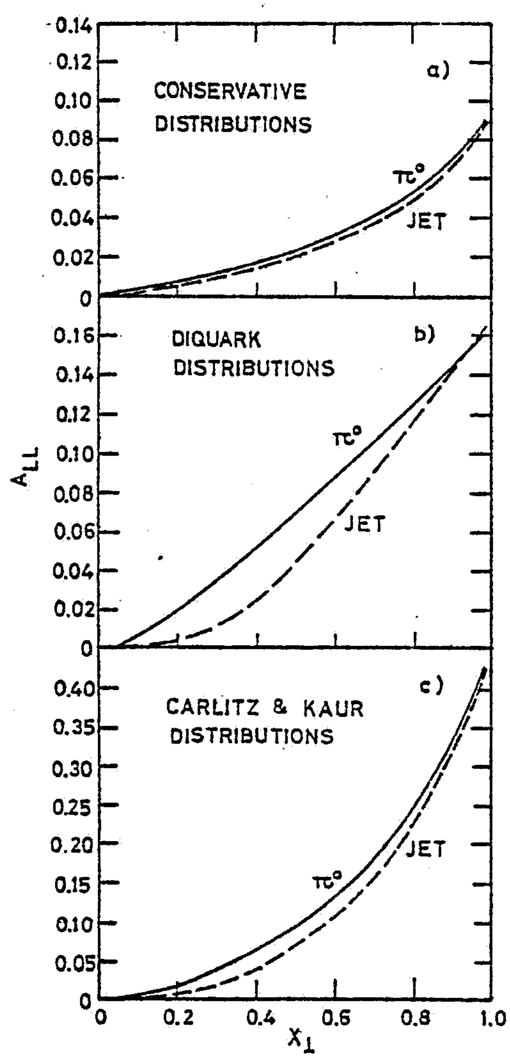

CONSERVATIVE DISTRIBUTIONS
a)
π°
JET
DIQUARK DISTRIBUTIONS
b)
CARLITZ & KAUR DISTRIBUTIONS
c)
A_LL
X_⊥

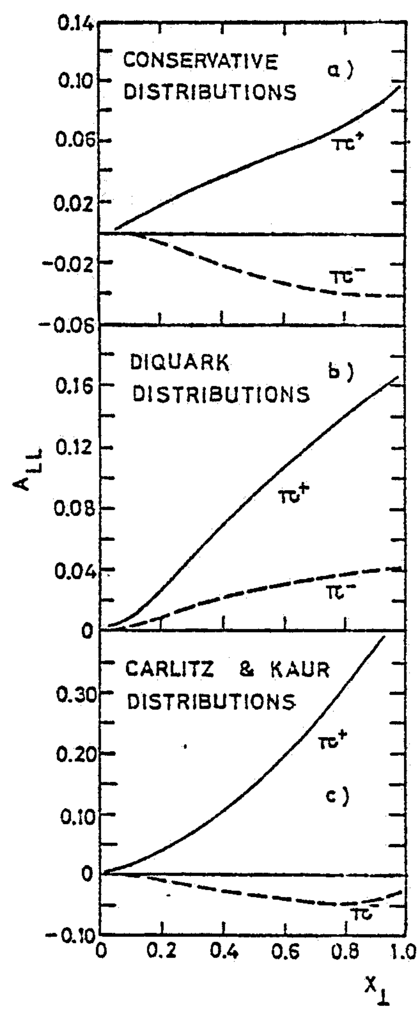

CONSERVATIVE DISTRIBUTIONS
a)
π⁺
π⁻
DIQUARK DISTRIBUTIONS
b)
CARLITZ & KAUR DISTRIBUTIONS
c)
A_LL
X_⊥

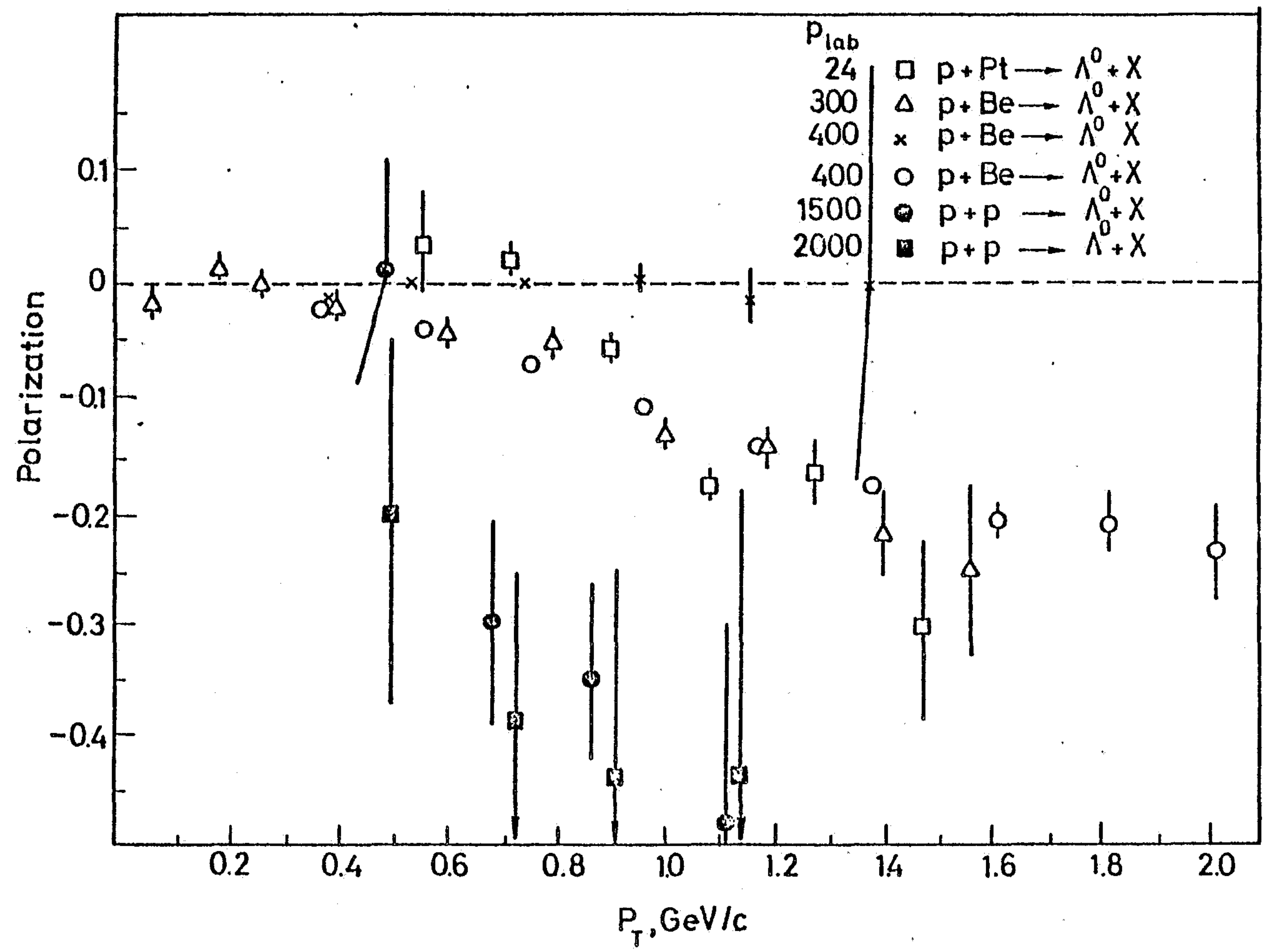

p_{lab}
24 □ p + Pt → Λ^0 + X
300 △ p + Be → Λ^0 + X
400 × p + Be → Λ^0 X
400 ○ p + Be → Λ^0 + X
1500 ● p + p → Λ^0 + X
2000 ■ p + p → Λ^0 + X
Polarization
0.1
0
-0.1
-0.2
-0.3
-0.4
0.2
0.4
0.6
0.8
1.0
1.2
1.4
1.6
1.8
2.0
P_T, GeV/c

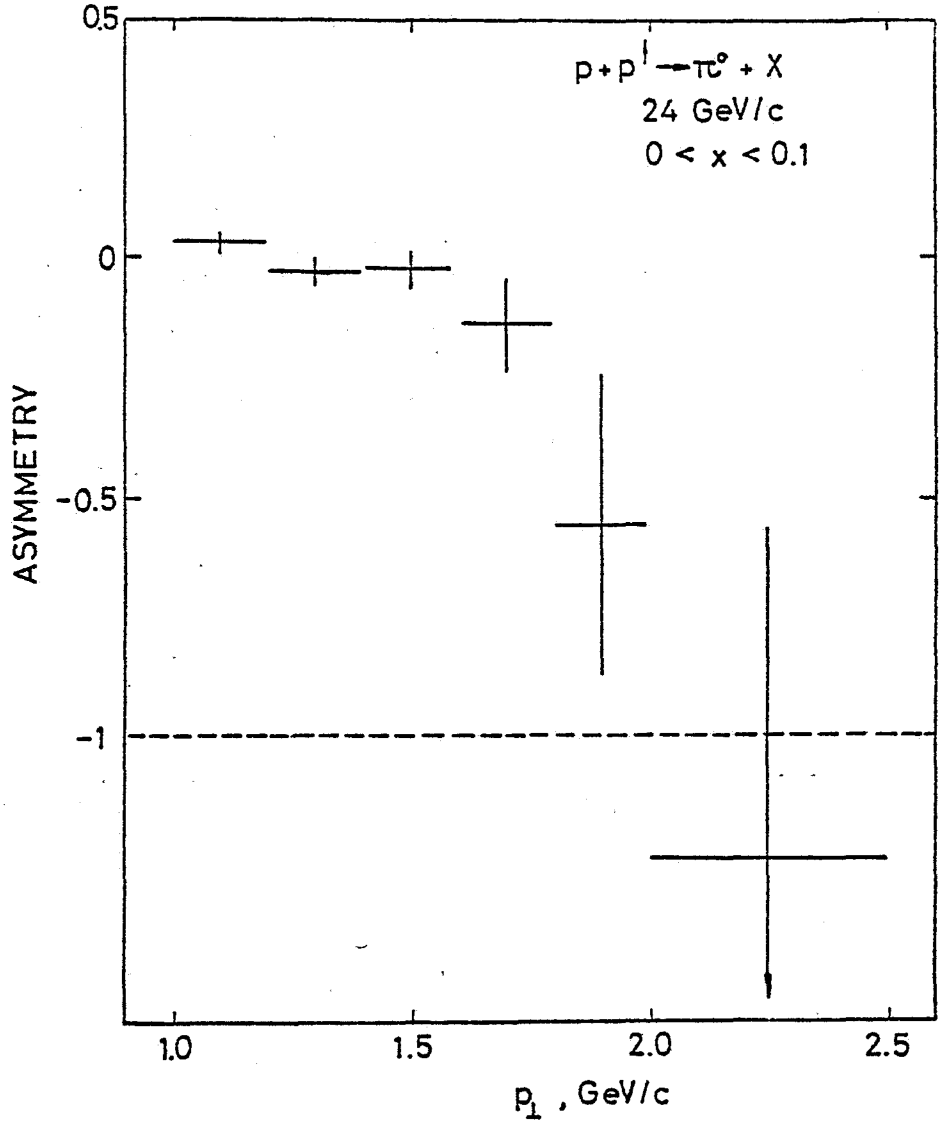

p + p↑ → π° + X
24 GeV/c
0 < x < 0.1
ASYMMETRY
0.5
0
-0.5
-1
1.0
1.5
2.0
2.5
p⊥ , GeV/c

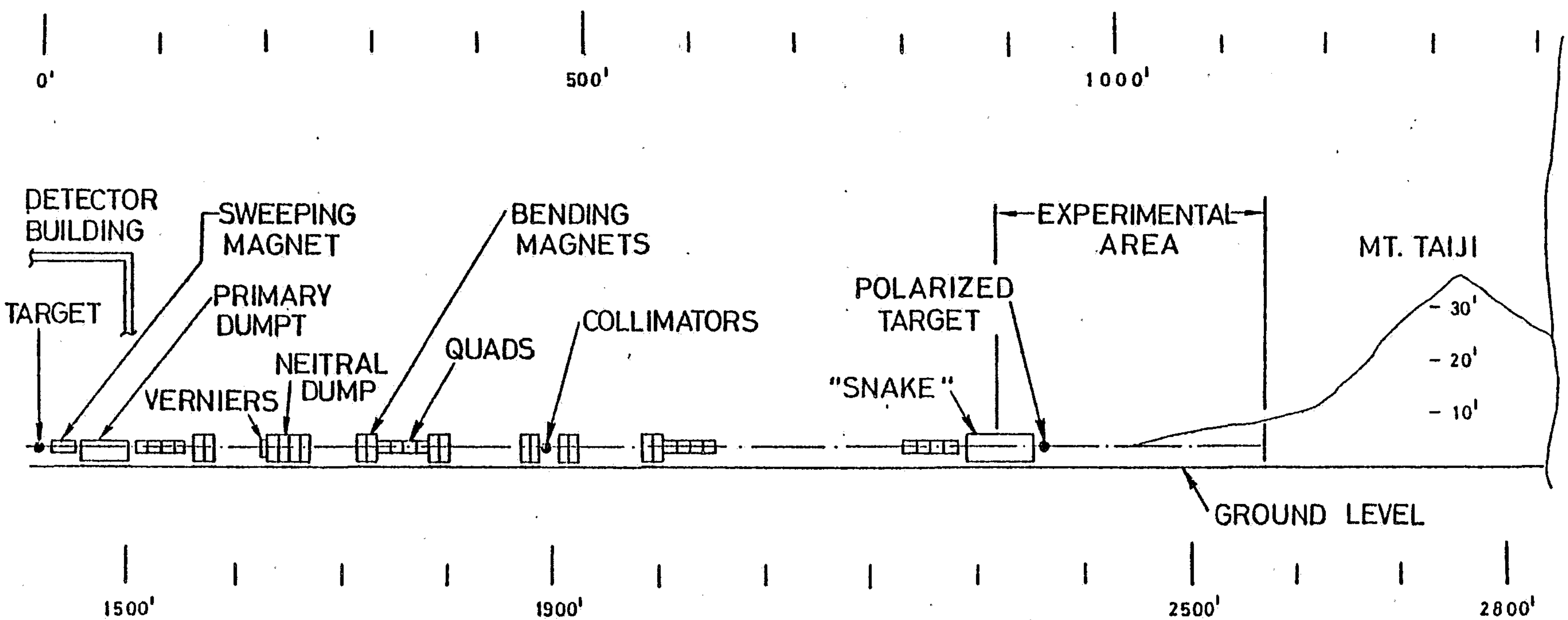

0'
500'
1000'
DETECTOR BUILDING
SWEEPING MAGNET
BENDING MAGNETS
EXPERIMENTAL AREA
MT. TAIJI
TARGET
PRIMARY DUMPT
POLARIZED TARGET
COLLIMATORS
30'
NEITRAL DUMP
QUADS
20'
VERNIERS
"SNAKE"
10'
GROUND LEVEL
1500'
1900'
2500'
2800'

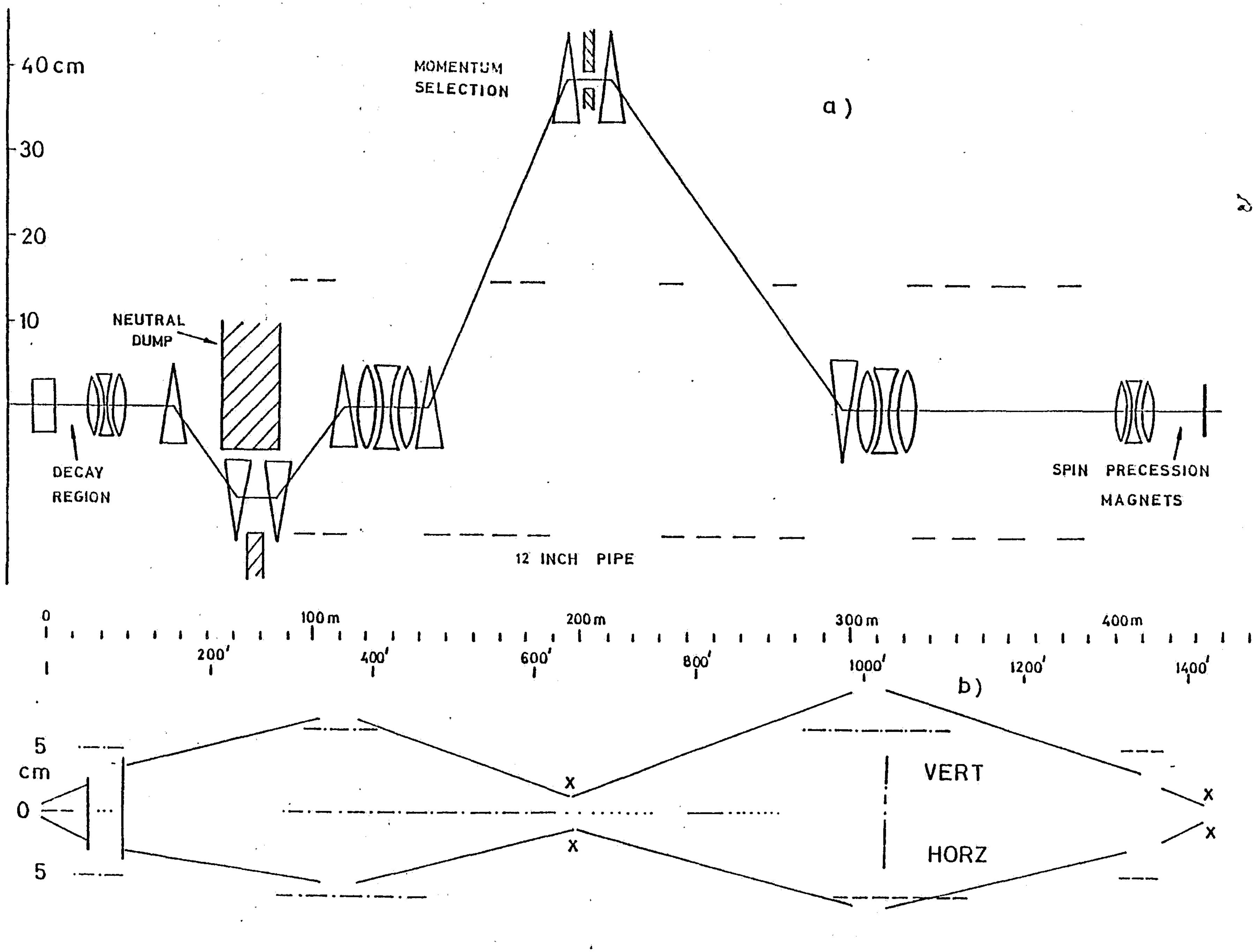

40 cm
30
20
10
MOMENTUM
SELECTION
a)
NEUTRAL
DUMP
DECAY
REGION
SPIN PRECESSION
MAGNETS
12 INCH PIPE
0
100 m
200 m
300 m
400 m
200'
400'
600'
800'
1000'
1200'
1400'
b)
5
cm
0
5
VERT
HORZ
x

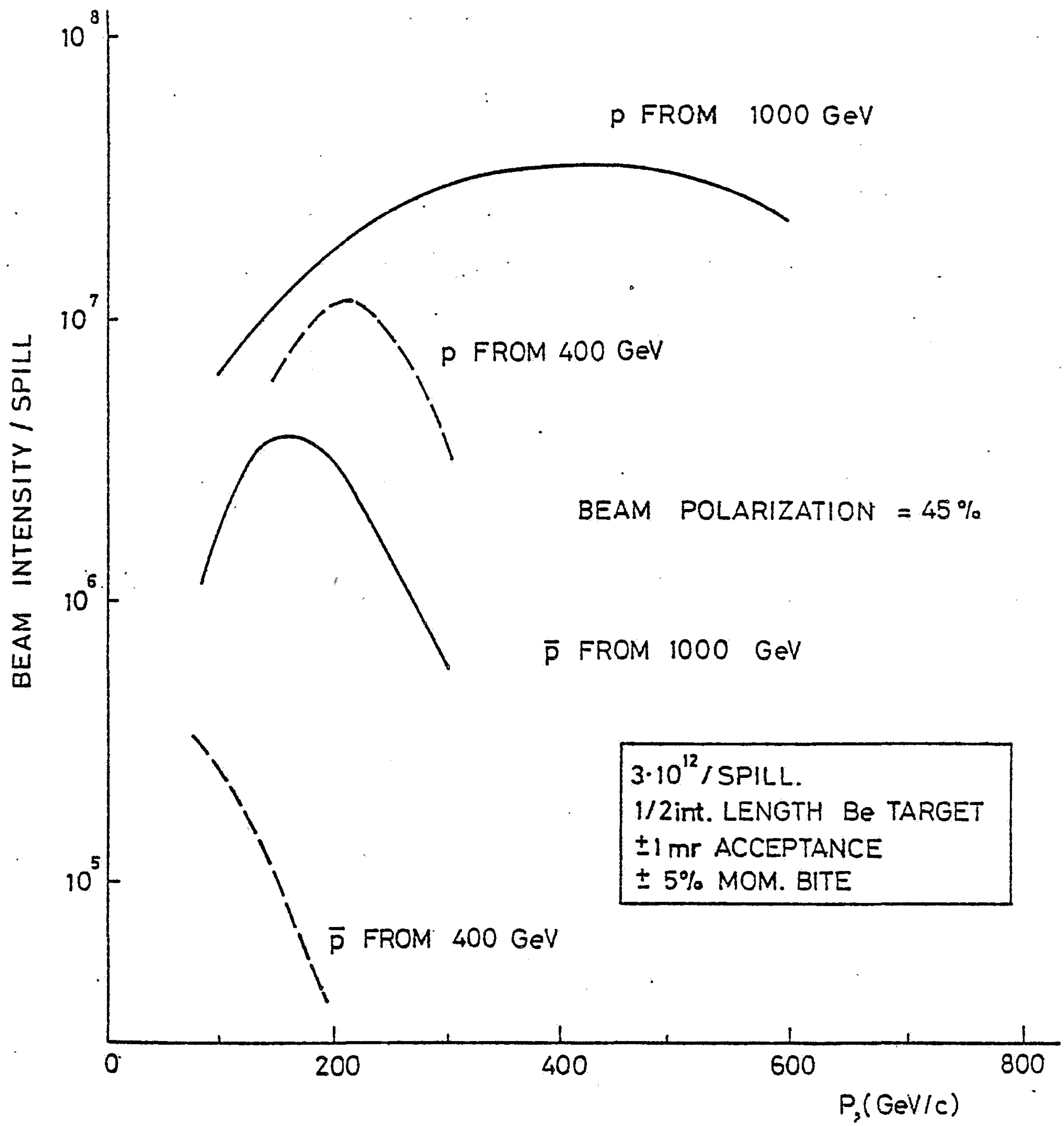

BEAM INTENSITY / SPILL
10^8
10^7
10^6
10^5
p FROM 1000 GeV
p FROM 400 GeV
BEAM POLARIZATION = 45 %
$\bar{p}$ FROM 1000 GeV
$\bar{p}$ FROM 400 GeV
$3 \cdot 10^{12}$ / SPILL.
1/2 int. LENGTH Be TARGET
±1 mr ACCEPTANCE
± 5% MOM. BITE
0
200
400
600
800
P, (GeV/c)

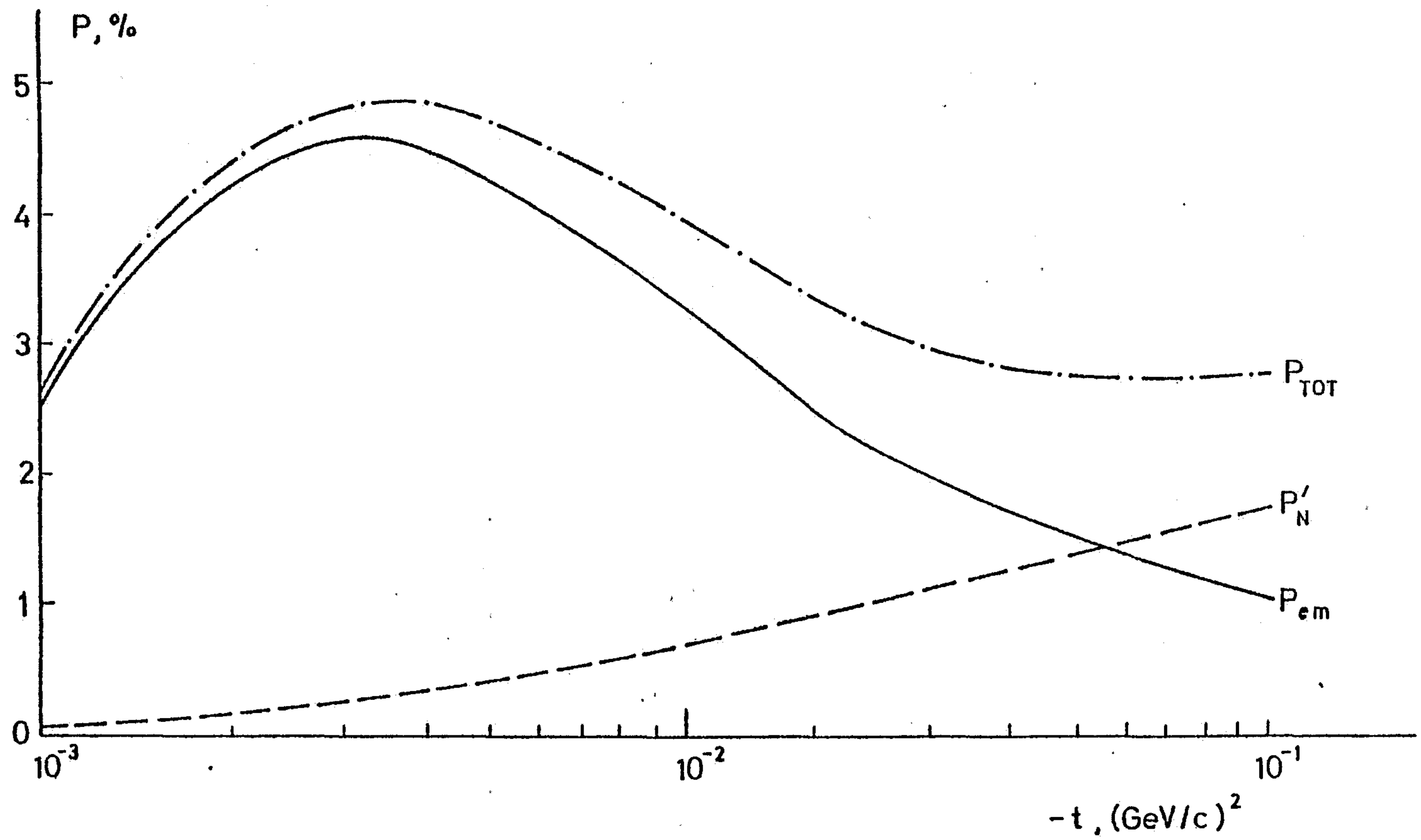

P, %
5
4
3
2
1
0
10^{-3}
10^{-2}
10^{-1}
$-t$, $(GeV/c)^2$
P_{TOT}
P'_N
P_{em}

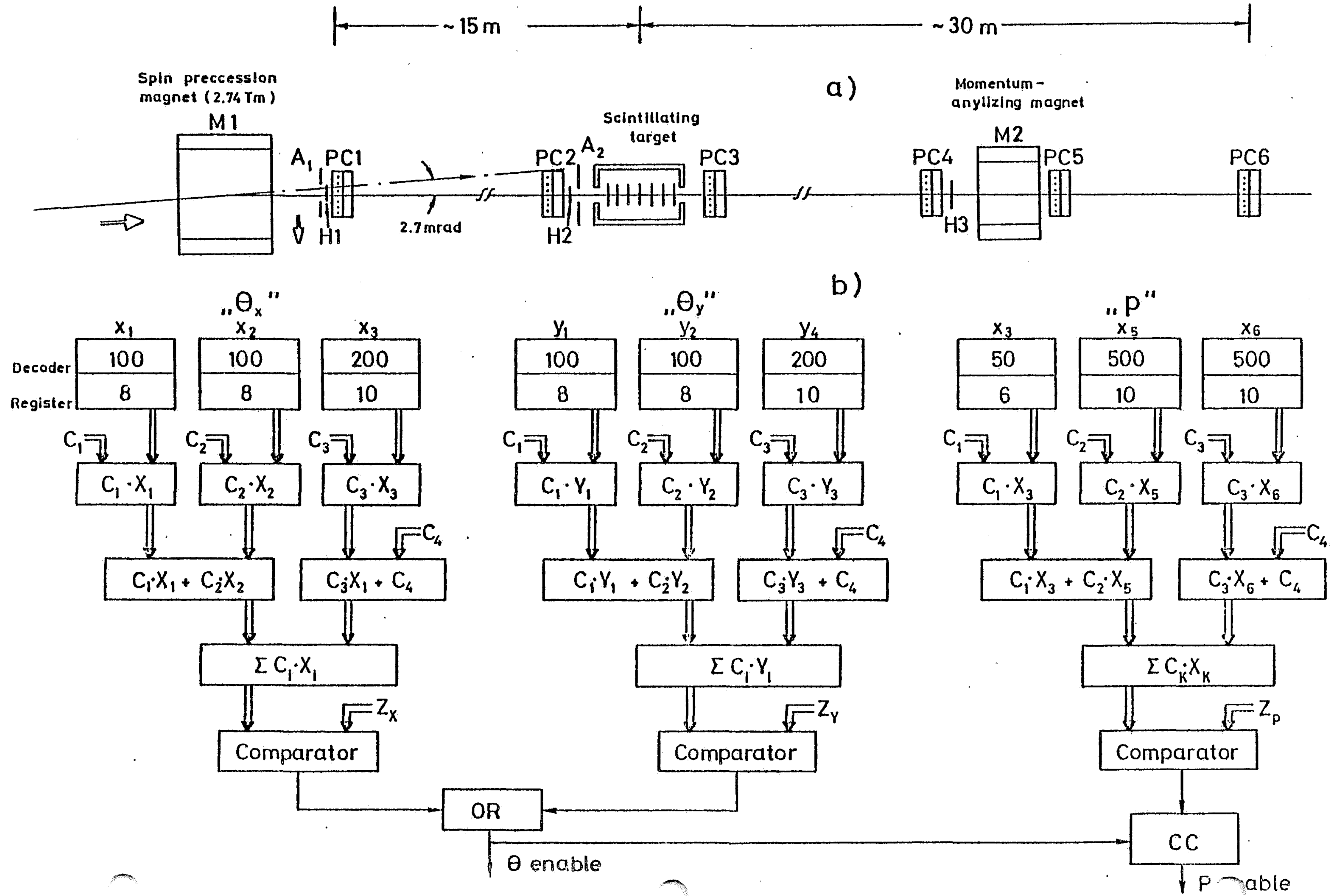

~15 m
~30 m
a)
Spin preccession magnet (2.74 Tm)
M1
A1
PC1
H1
2.7mrad
PC2
A2
H2
Scintillating target
PC3
Momentum - anylizing magnet
M2
PC4
H3
PC5
PC6
b)
„Θx"
„Θy"
„p"
Decoder
Register
x1 100 8
x2 100 8
x3 200 10
y1 100 8
y2 100 8
y4 200 10
x3 50 6
x5 500 10
x6 500 10
C1 · X1
C2 · X2
C3 · X3
C1 · Y1
C2 · Y2
C3 · Y3
C1 · X3
C2 · X5
C3 · X6
C1·X1 + C2·X2
C3X1 + C4
C1·Y1 + C2·Y2
C3·Y3 + C4
C1·X3 + C2·X5
C3·X6 + C4
Σ Ci·Xi
Σ Ci·Yi
Σ CK·XK
Zx
Zy
Zp
Comparator
Comparator
Comparator
OR
CC
θ enable
P enable

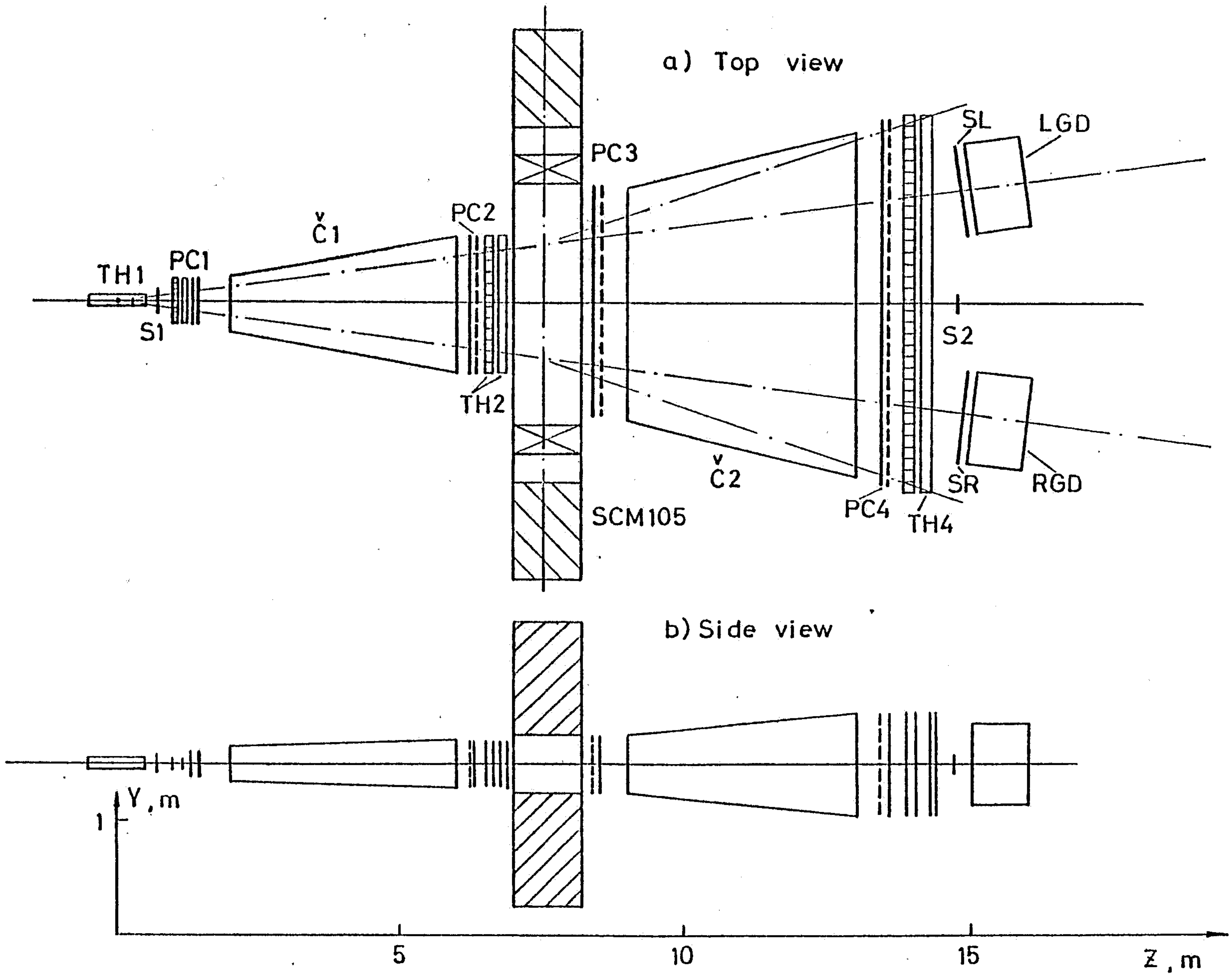

a) Top view
TH1
S1
PC1
Č1
PC2
TH2
PC3
SCM105
Č2
PC4
TH4
SL
LGD
S2
SR
RGD
b) Side view
Y, m
1
5
10
15
Z, m

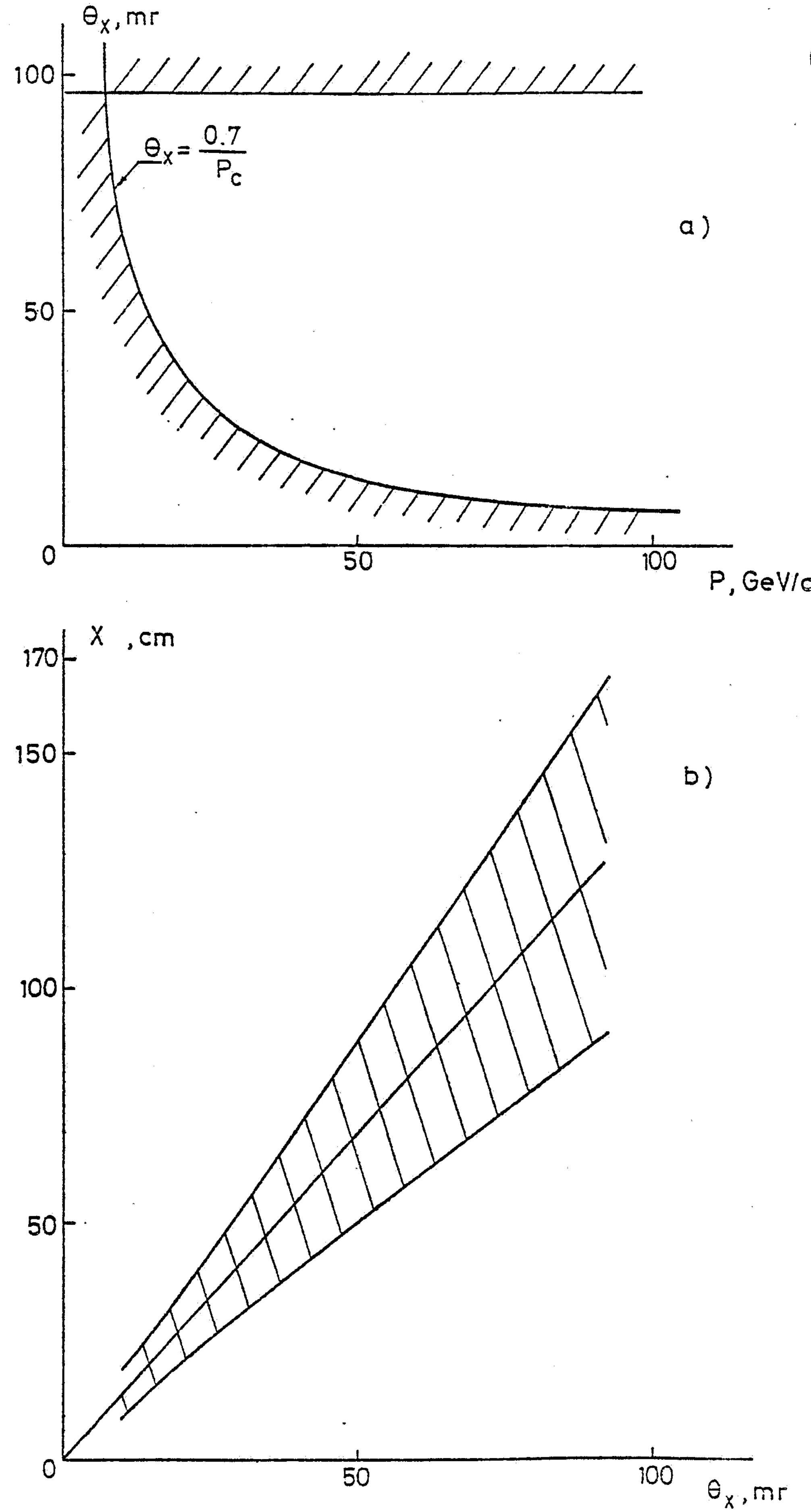

θx, mr
100
50
0
θx = 0.7/Pc
a)
50
100
P, GeV/c
X , cm
170
150
100
50
0
b)
50
100
θx, mr

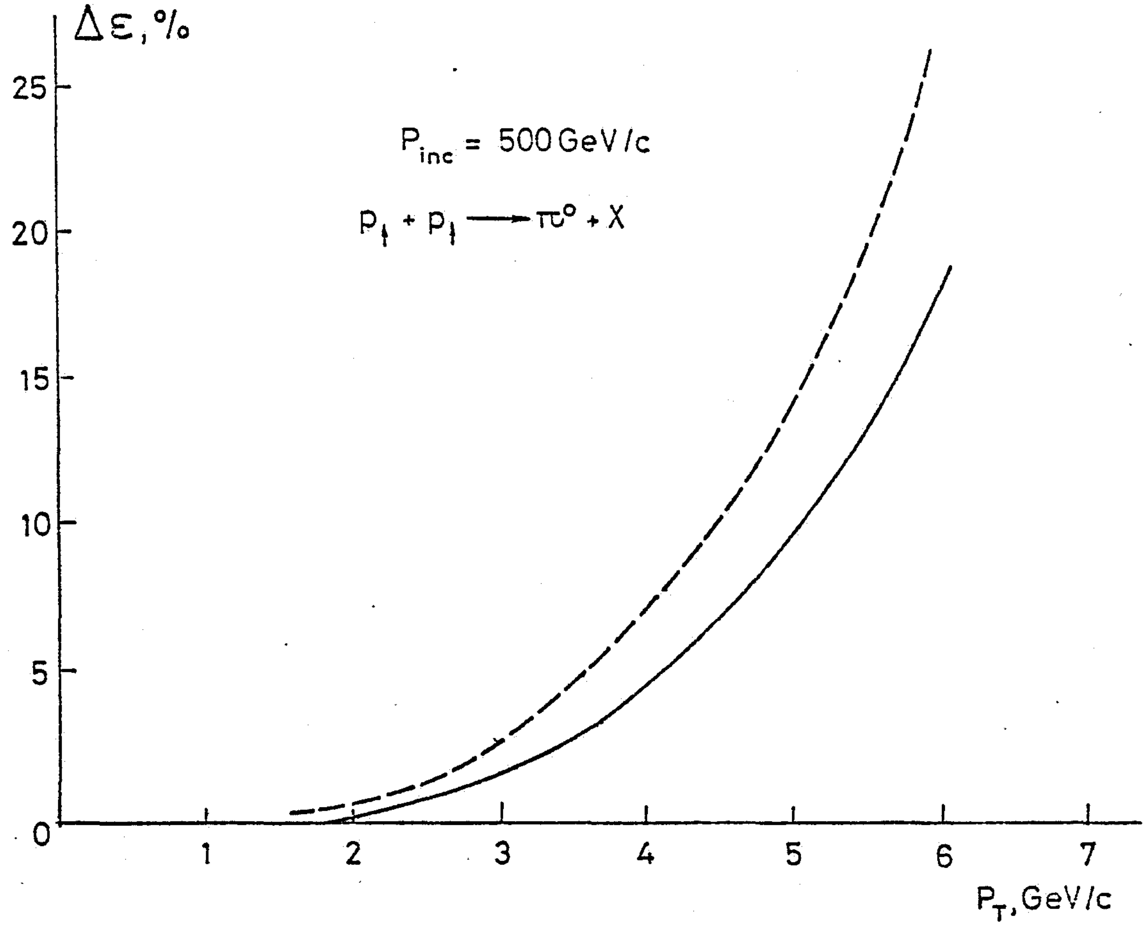

Δε, %
25
20
15
10
5
0
P_{inc} = 500 GeV/c
$p_{\uparrow} + p_{\uparrow} \longrightarrow \pi^0 + X$
1
2
3
4
5
6
7
P_T, GeV/c

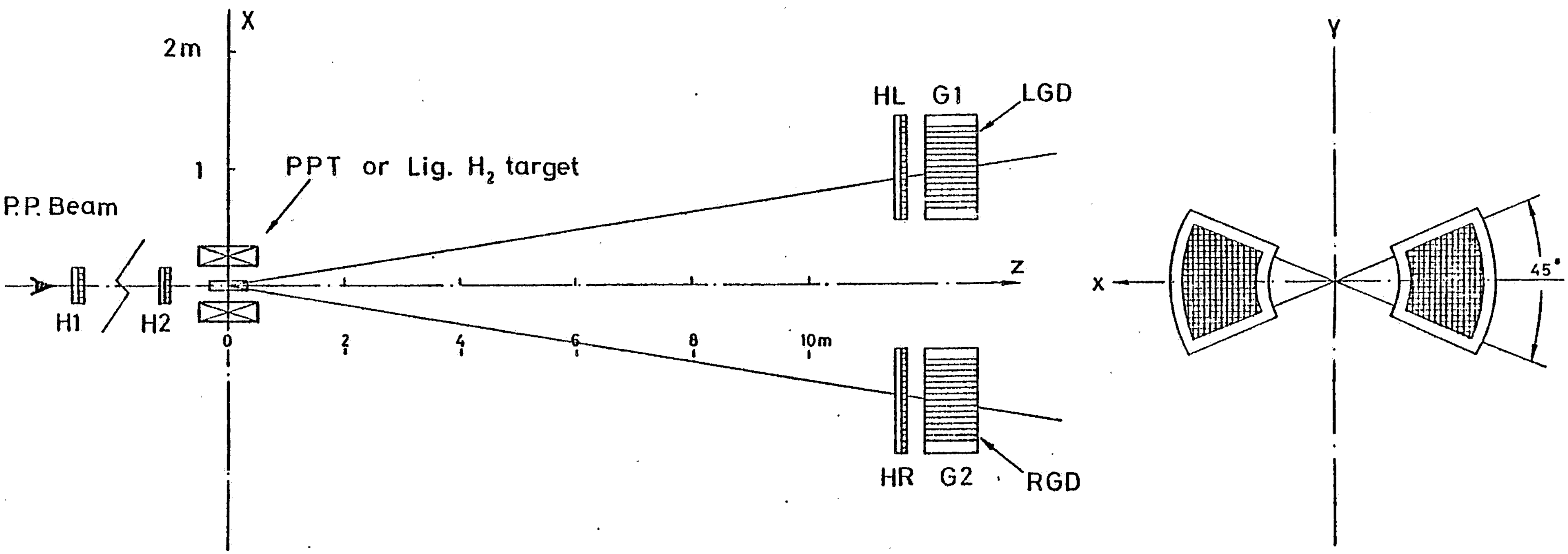
X
2m
1
P.P. Beam
PPT or Liq. H_2 target
H1
H2
0
2
4
6
8
10m
Z
HL
G1
LGD
HR
G2
RGD
Y
X
45°

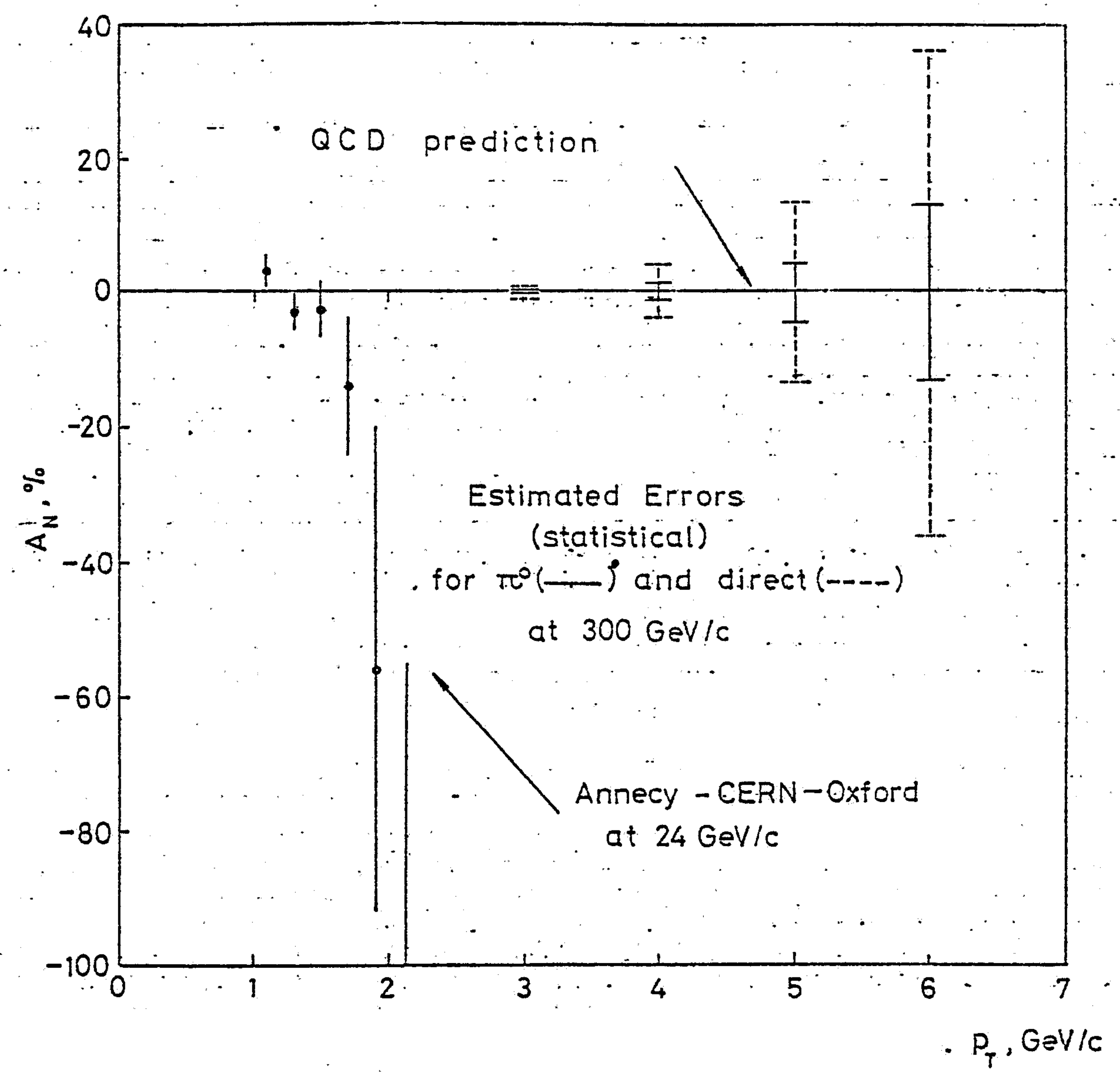

QCD prediction
Estimated Errors
(statistical)
for π° (——) and direct (----)
at 300 GeV/c
Annecy - CERN - Oxford
at 24 GeV/c
A_N, %
p_T, GeV/c
40
20
0
-20
-40
-60
-80
-100
0
1
2
3
4
5
6
7

Proposal to Study the Spin Dependence in Inclusive π^0 and Direct-Gamma Production at High $p_\perp$ with the Polarized Proton Beam Facility at Fermilab

by

CEN-Saclay, LAPP-Annecy, INFN-Trieste,
Kyoto University, Kyoto-Sangyo University, Kyoto University of Education,
Hiroshima University, University of O.E.H. (Kita-Kyushu),
Argonne National Laboratory, Fermi National Accelerator Laboratory,
University of Iowa, Los Alamos National Laboratory,
Northwestern University, Rice University, IHEP-Serpukhov,
University of Udine Collaboration*

31 March 1989

Preface

Part of P-678 was included in E-704 following the PAC's recommendations in 1981. In E-704, we explore a relatively lower region of $p_\perp$ in the π^0 production. On March 8, 1989, there was a meeting with the Fermilab management to discuss the status of the electromagnetic calorimeter for the polarized-beam experiments. During the meeting it was suggested that we update P-678 before the April PAC meeting. Although studies on the single-gamma measurements are continuing, we consider this P-678 update to be reasonably adequate. We are also counting on learning many facts about π^0 detection, which relates to direct-gamma detection, during the forthcoming E-704 run.

---

* Individual names are likely to be similar to the present participants in E-704. Precise list will be presented later.

Scientific Spokesman: Sergei Nurushev, IHEP - Serpukhov
Deputy Spokesman: K. Kuroda, LAPP - Annecy

ABSTRACT

We propose to measure the single-spin asymmetry parameter A_N in inclusive π° production at high $p_\perp$ and direct-γ production using the polarized proton-beam facility at Fermilab. In addition, we propose to measure the double-spin asymmetry parameter A_{LL} in inclusive π° production and direct-γ production using a polarized ^{6}LiD target.

A number of lead-glass counters will be doubled compared with existing E-704 electromagnetic calorimeter in order to gain rate and improve misidentification problems.

I. Introduction

Asymmetry measurements in π° production yield a value as large as A_N = 60% in the 2 < $p_\perp$ < 3 GeV/c region measured at 24 GeV/c (CERN) and 40 GeV/c (Serpukhov).[1] It seems important to pursue measurements to higher values of $p_\perp$ in order to investigate the spin dependence in the hard scattering of hadronic constituents. Simultaneously, the asymmetry in direct-γ production can be measured where A_N = 0 is expected by QCD perturbative theory.

Results of new measurements by the EMC group at CERN have been interpreted to mean that the proton spin may not be due to the helicity of its constituent quarks. Most of the proton spin may be due to gluons and/or orbital angular momentum. To understand the basic question of the origin of proton spin, π° and direct-γ production measurements at high $p_\perp$ with longitudinally polarized protons on longitudinally polarized target protons seem to be very desirable.[1]

The QCD Compton effect, gluon + quark → gamma + quark, is expected to be the dominant mechanism for direct-γ production at large $p_\perp$. In contrast to the π°, which represents only a fragment of the scattered constituent, the γ

itself participates directly in the hard-scattering process. As a direct consequence the ratio γ/π° should increase with increasing $p_\perp$, this prediction has been confirmed in several different experiments.[3] Thus, direct-γ production provides a particularly clean process for studying the dynamics of hadronic constituents without the complexities of quark fragmentation.

Although important qualitative features may be deduced from single-spin asymmetry measurements, the study of double-spin asymmetries can provide quantitative insight into the spin properties of gluons which are not accessible to deep-inelastic ep scattering experiments. The double-spin asymmetry A_{LL} in inclusive π° and direct-γ production has been estimated by several authors.[2,4]

We propose to study spin dependence in the reactions

$$p + p \rightarrow \pi^\circ + \text{anything}, \qquad (1)$$

and

$$p + p \rightarrow \gamma + \text{anything} \qquad (2)$$

with emphasis on the high-$p_\perp$ region (up to 6 GeV/c). The quantities to be measured are the single-spin asymmetries

$$A_N = \frac{Ed^3\sigma(\uparrow)/dp^3 - Ed^3\sigma(\downarrow)/dp^3}{Ed^3\sigma(\uparrow)/dp^3 + Ed^3\sigma(\downarrow)/dp^3} \qquad (3)$$

for both reactions (1) and (2) with a transversely polarized proton beam and liquid hydrogen (H_2) target. In addition we propose to measure the double-spin asymmetry for (1) and (2).

$$A_{LL} = \frac{Ed^3\sigma(++)/dp^3 - Ed^3\sigma(+-)/dp^3}{Ed^3\sigma(++)/dp^3 + Ed^3\sigma(+-)/dp^3} \qquad (4)$$

where ++(+-) indicate parallel (antiparallel) helicities for longitudinally polarized beam and target protons. This measurement requires replacement of the liquid H_2 target by a polarized ^{6}LiD target.

Major changes in this proposal from the E-704 setup are: i) doubled lead-glass counters, ii) polarized ^{6}LiD target, and iii) installation of guard counters surrounding the lead-glass counters.

II. Experimental Methods

A. Experimental Arrangement

A schematic view of the experimental arrangement is shown in Fig. 1. The polarized proton beam enters from the left. Trajectories of individual beam particles are defined by hodoscopes H_{B1} and H_{B2}; these are separated by 20 meters and have spatial resolutions of 1.5 mm in both the x and y directions. For single-spin measurements a liquid H_2 target 100-cm long will be used with the proton beam transversely polarized. For the double-spin asymmetry measurements the longitudinally polarized proton beam will be incident on a longitudinally polarized ^{6}LiD target. The proposed snake system will allow the beam polarization to be frequently flipped with no important change in beam geometry.

Photons from the decay of π^0's produced by the interaction of protons on either a LH_2 or polarized target are detected in the two Pb-glass calorimeters G_1 and G_2 (called "CEMC", central electromagnetic calorimeter) consisting of 2016 cells as shown in Fig. 1. The number of lead-glass in the present E-704 CEMC (1008 cells) will be doubled. At p_{in} = 200 GeV/c the CEMC is placed 10 m downstream of the target and centered around θ = 97 mrad which corresponds to x_F = 0. The azimuthal angle subtended by each calorimeter is $\pm$ 45° with respect to the horizontal plane.

The proportional chambers placed between the target and the CEMC serve to localize charged particles which accompany γ's and assure no charged tracks in the γ direction. To improve background identification in direct-γ production, the CEMC is provided with additional γ detectors G_1' and G_2' as shown in Fig. 1. These additional counters ensure identification of π° and η° decays in which only one γ falls within the fiducial area of the CEMC.

The acceptance of the detector in x_F-$p_\perp$ space in shown in Fig. 2 for p_{in} = 200 GeV/c.

B. Electromagnetic Calorimeters

The electromagnetic calorimeters (CEMC) comprise a major part of the detector. Each consists of 1008 Pb-glass cells (3.8 x 3.8 x 45 cm) stacked to form a trapezoidal array as shown in Fig. 3. The Cerenkov light is collected by a photomultiplier at the rear of each cell. (The detector elements and the design of the associated electronic system are similar to those developed by the IHEP-IFSN-LAPP Collaboration for the GAMS 4000 spectrometer at CERN.)

The principal characteristics of P-678 CEMC are listed in Table I. This detector has shown remarkable spatial resolution (± 1 mm at 100 GeV), resulting from an optimal choice of tranverse dimensions of the Pb-glass cells.

To accommodate high event rates the integrated charge in each cell is digitized with its own ADC. Pedestal subtraction and energy normalization are performed automatically by a fast processor. Relative gains (PM + ADC) will be monitored with an LED system between spills. The energy resolution has been measured during the last fixed-target run; at full width half-maximum (FWHM) it is

$$\Delta E/E = 0.024 + 0.12/\sqrt{E}\ (\mathrm{GeV})$$

giving ± 2.5% at 25 GeV. Linearity has been studied with electrons from 30 to 40 GeV, and no deviation larger than 1% was observed.

Energies and coordinates (using the method of moments) will be evaluated on-line. This provides the possibility for on-line calculation of gamma-gamma invariant mass and kinematics, and allows one to impose event selection criteria if necessary before recording data on tape. With reasonable estimates for processing times we conclude that as many as 500 events/sec can be recorded even with large multiplicities.

C. Identification of π^0 Events

It is apparent, however, that event rejection is preferably executed off-line after careful study so that no bias is introduced in the inclusive final states.

To obtain a 'clean' sample of π^0 events all data must be subjected to extensive off-line analysis. Backgrounds due to improperly paired γ's will be estimated using the LUND Monte Carlo (PYTHIA) simulation. Contamination of the final sample by π^0's from decay of inclusively produced η's, ω^0's, and K_s^0's can be reasonably estimated from available measurements and LUND Monte Carlo calculations which relate charged and neutral production. This contamination will be small at high $p_\perp$.

D. Identification of Direct-γ Events

The problems involved in identification of direct-γ's in a background of π^0 decays have recently been addressed with considerable success.[3] Background arises from

i) The decays $\pi^0 \rightarrow \gamma\gamma$ and $\eta \rightarrow \gamma\gamma$ in which one γ misses a spectrometer, is below threshold for detection, converts in the target, or the two γ's are too closely spaced to be geometrically resolved.

ii) We assumed that a background of η decays is negligible compared with π° based on the UA6 experiment.[3] Additional comments are made on page 9.

iii) Neutral hadrons such as n, $\bar{n}$, or $K_L{}^\circ$ which interact in the Pb-glass and a simulate a single shower.

In order to see the feasibility of the high-$p_\perp$ single-γ measurements, two cases (see a and b below) of fake single γ sources, and the single-gamma detection efficiency (see c) have been studied by Monte Carlo simulation. A coarse calorimeter surrounding the CEMC is discussed (see d). π° conversions in the polarized target is estimated (see e).

a) Two γ's from a π° are misidentified with a single energy cluster on the calorimeter even though both γ's hit the CEMC.

The CEMC is placed at z = 1000 cm as above. The electromagnetic showers were generated using the GEANT3 software package. The energy clusters in the CEMC were reconstructed using software developed by the Serpukhov group. The reconstruction was made with a certain energy threshold for each energy cluster, because we would have to set such an energy threshold in the off-line analysis for the real events in order to avoid noise signals. If two γ's are too close in space (e.g. as close as 3 cm at $p_\perp$ = 5.5 GeV/c), then the present reconstruction program tends to fail to divide the energy properly between two γ's. The mass reconstruction becomes worse in such cases. However, the program can tell whether the shower consists of a single-γ or multiple-γs with a minimum of two γ separation of $\sim$ 2cm by checking the shower shape. One ADC channel corresponds to 0.02 GeV, and we expect the noise level to be about 0.1 GeV or less. The ratio of this type of fake single γ's over π°'s is estimated to be below 1.7% throughout the $p_\perp$ range from 2.5 to 5.5 GeV/c. This is lower than the direct-γ production rate.

b) One γ from a π° hits the CEMC with high-$p_{\perp}$ and the other misses the lead-glass.

The background events in which one γ from a π° hits the CEMC with high-$p_{\perp}$ and the other γ misses the CEMC can be reduced by placing a surrounding coarse calorimeter around the CEMC. Figure 4 shows the fraction of π° events for which a gamma is missed and found in the surrounding calorimeter. The γ's hitting the surrounding calorimeter have low energies; about 30% of such γ's have an energy less than 0.6 GeV, because the γ's hitting the CEMC have to carry much larger fractions of the parent π° energies to clear the $p_{\perp}$-threshold.

Figure 5 shows the resulting fake direct-gamma spectrum. This includes the fact that the remaining gamma is lower energy (and $p_{\perp}$) than the π°, giving approximately an additional order of magnitude suppression in rate at a given $p_{\perp}$. The resulting background is about 1% of the π° rate at a given $p_{\perp}$. It also includes loss of one gamma due to conversions in the target material as mentioned in point e.

Therefore, it is nice to have the surrounding calorimeter as illustrated in Fig. 4 but not absolutely necessary.

Preliminary studies for similar problems due to missing one gamma from η decays have been done. These indicate no serious problem above $p_{\perp}$ of 1.5 GeV/c.

c) Direct photon and accompanying photon(s)

Multiple γ's entering the CEMC with real single-γ events are estimated to be about 10% of real events. Figure 6 shows the probability of direct photon without accompanying photon(s) in either the CEMC or the surrounding calorimeter estimated by the LUND (PYTHIA) Monte Carlo.

d) Coarse electromagnetic calorimeters G_1' and G_2' surrounding the CEMC will likely be segmented lead-sandwiched scintillators. The detector is currently being designed.

e) Another source of single gamma background from conversions in the target

The target is about 26% of a radiation length and the vacuum shells about 4%. As discussed above, the remaining gamma is of lower energy than the π° and so the background spectrum is only 1% of the π° spectrum at a given $p_\perp$. This is included in Fig. 5.

The neutral hadron contribution to background will be measured in a separate run using the method of Cox et al.[5] Ten radiation lengths of Pb will be inserted in the space between the proportional chambers and the Pb-glass spectrometers. The γ flux is largely degraded while the neutral hadronic component is attenuated only 30% due to interactions in the Pb. This background varies depending on the kinematic region and therefore must be subtracted separately in each X_F and $p_\perp$ interval.

The inclusive π°'s and direct-γ's will be carried out simultaneously for both A_N and A_{LL} measurements.

E. Polarized ^{6}LiD Target

It was recently established[6] that substantial nuclear polarizations can be achieved in large targets of ^{6}LiD. To the extent that $^6Li^\uparrow$ can be viewed as $\alpha + D^\uparrow$, fully one-half of the nucleons are polarized in such a material. Polarizations of $^6Li^\uparrow$ and $D^\uparrow$ approaching 70% should be achievable in the MP-9 polarized target, with the addition of a high-frequency (180 GHz) microwave source.

III. Rate and Error Estimate

Rates for π° and γ production have been estimated with the following assumptions:

Primary Beam: $4 \cdot 10^{12}$ incident protons/spill

Beam Momentum: 200 GeV/c

Beam Intensity: 3×10^7/spill with 1 spill/60 sec, and polarization $P_B = 0.45$

Geometrical Efficiency for π° detection = 0.25

Geometrical Efficiency for γ detection = 0.50

Liquid H_2 target: 100-cm long for A_N measurements

Polarized ^{6}LiD target ($\alpha + 2p^\uparrow + 2n^\uparrow$): 20-cm long for A_{LL} measurements

A) A_N Measurement

The invariant cross section for π° production was calculated with the parametrization of R. M. Baltrusaitis et al. [7]

$$f = E\frac{d^3\sigma}{d^3p} = A\ P_\perp^{-N}\ (1-X_R)^M,$$

where $X_R = \sqrt{X_F^2 + X_\perp^2}$, $A = 3.12 \times 10^{-27}$ cm^2/GeV^2, $M = 4.81$, $N = 8.9$. The results are given in Table 2 for an integrated beam intensity of 1.8×10^{12} polarized protons corresponding to 1000 hours running time.

The statistical error in A_N is

$$\Delta A_N \approx \frac{\sqrt{\chi}}{P_B}\ \frac{1}{\sqrt{N_{Tot}}},$$

where $\chi = 1 + \frac{B}{S}$ and B/S = background over signal ratio.

In this case the backgrounds result largely from pairs of uncorrelated γ's which fall within the π°-acceptance criteria. This background can be estimated from the 2γ effective-mass distributions. With $\chi = 1.1$ as a reasonable estimate we obtain the errors ΔA_N given in Table II.

A similar estimate has been made for ΔA_N in direct-γ production. In this case it was assumed that the ratio γ/π° varied from 1/20 at $p_\perp = 3$ GeV/c to 1/10 at $p_\perp = 5$ GeV/c. With the assumption $\chi \simeq 1.5$ we obtain the estimated statistical errors given in Table III.

B) <u>A_{LL} Measurement</u>

The double-spin asymmetry measurements require both polarized beam and target. The statistical error may be approximated

$$\Delta A_{LL} \simeq \frac{\sqrt{\chi}\ \alpha}{P_B P_T} \frac{1}{\sqrt{N_{Tot}}}$$

here the 'polarization dilution factor' α reflects production on unpolarized target constituents. This factor depends not only on the target material but also on the kinematic conditions, particularly $p_\perp$. To estimate ΔA_{LL} we assumed that $\alpha \approx 2$ to 3 as $p_\perp$ increases from 2-5 GeV/c. For the double-spin asymmetry we obtain the errors ΔA_{LL} given in Tables IV and V for $pp \to \pi^\circ X$ and $pp \to \gamma X$, respectively.

SYSTEMATIC ERRORS:

The systematic errors divide roughly into multiplicative and additive. Uncertainties in target and beam polarizations are multiplicative errors. Target polarization can be measured to $\pm$ 3% with the principal uncertainty in calibration of the nuclear magnetic resonance system which uses the thermal equilibrium signal. It is estimated that beam polarization can be calculated to $\pm$ 3% from the beam optics.

Additive errors which may introduce a spurious asymmetry in the data can arise from

i) changes in beam geometry with reversal of beam polarization

ii) misalignment of detector components

iii) changes in gain of spectrometer elements.

Geometric sources of error associated with either the beam or detector can be accurately controlled through frequent cross-checks of counting rates with different spin-spin and spin-detector (right or left) combinations. With frequent reversals of beam polarization long-term variations in gain will be averaged out.

IV) Beam Time Request

1) 250 hours for beam polarization studies by polarimeters

2) 250 hours for lead-glass calibration

3) 1000 hours for $A_N(p^{\uparrow}p \to \pi^{\circ}X)$ and $A_N(p^{\uparrow}p \to \gamma X)$

4) 1000 hours for $A_{LL}(p^{\uparrow}p^{\uparrow} \to \pi^{\circ}\ X)$ and $A_{LL}(p^{\uparrow}p \to \gamma X)$

We will be ready to carry out these measurements during the next-fixed target period (not forthcoming) and likely before E-704 follow up (two-spin hyperon production measurement, to be specified).

V) Additional Equipment Needs Beyond E-704

Lead-glass counters, phototubes and bases	Serpukhov
Electronics, mainly fast bus ADC and H.V. power supplies (60K + 100K)	Argonne and Fermilab
^{6}LiD target	Argonne, Saclay, Los Alamos
Gamma detector surrounding the CEMC	Shared by collaboration
Cables and connectors (signal and H.V.)	Fermilab

VI Special Remarks

Energy Upgrade

We would like to point out the importance of the MP-beam energy upgrade. In general, we would like to investigate the energy dependence of various reactions studied in E-704 from 200 to 500 GeV/c. We specifically describe the advantages at higher energies concerning this proposal.

i) Direct-gamma production cross section at high $p_\perp$ increases rapidly with energy; from 200 to 500 there is more than a one-order increase. This will allow us to cover higher $p_\perp$ region.

ii) For the study of gluon spin distribution, we need to cover low $X_\perp$ region ($X_\perp = 2p_\perp/\sqrt{s}$) at high $p_\perp$ and high s. We can reach $X_\perp$ = 0.3 (at $p_\perp$ = 5 GeV) at 500 GeV.

Polarized ^{7}LiH Target

We plan to propose a similar measurement with a polarized ^{7}LiH target to investigate possible differences in effect due to polarized proton and polarized neutron.

REFERENCES

1) A. N. Vasiliev, Proceedings of the Symposium on High Energy Spin Physics, Minneapolis, Minnesota, September, 1988.

2) This topic was extensively described during the Fermilab Polarization Symposium, June 1988 (See Proceedings of the Symposium on Future Polarization Physics at Fermilab); S. Brodsky et al., Phys. Lett. (1988); E. L. Berger and J. Qiu, to be published.

3) For instance, see A. Bernasconi et al., Phys. Lett. 206, 163 (1988); T. Ferbel and W. R. Molzen, Rev. of Mod. Phys. 56, No. 2, Part 1, 181 (1984).

4) M. B. Einhorn and J. Soffer, Nucl. Phys. 274, 714 (1986); N. S. Craigie, K. Hidaka, M. Jacob, and F. M. Renard, Phys. Reports, 99, 143 (1983), and references therein.

5) B. Cox et al., Proc. 1979 Int. Symp. on Lepton and Photon Interactions at High Energies, Fermilab, Batavia, p. 602.

6) P. Chaumette et al., Proceedings of the Symposium on High Energy Spin Physics, Minneapolis, Minnesota, September, 1988.

7) R. M. Baltrusaitis et al., Phys. Rev. Lett. 44, 122 (1980).

8) K. Hidaka, private communication.

9) M. J. Alguard et al., Phys. Rev. Lett. 37, 1261 (1976); 41, 70 (1978); G. Baum et al., Phys. Rev. Lett. 51, 1135 (1983).

10) J. Ashman et al., (European Muon Collaboration), Phys. Lett. B206, 364 (1988).

APPENDIX

A_{LL} Measurement and Gluon Spin Distribution

We describe here how to determine the gluon polarization by measuring the parameter A_{LL} in direct-gamma production, $p^{\uparrow}p^{\uparrow} \rightarrow \gamma + X$ (a polarized beam on a polarized-proton target).

To good approximations for $x_{\perp} \gtrsim 0.1$,[4]

$$A_{LL}\ (x_F = 0,\ x_{\perp}) \simeq [\Delta U(X_{\perp})/U(X_{\perp})] \cdot [\Delta V(X_{\perp})/V(X_{\perp})] \cdot \hat{A}_{LL}^{UV}\ (\hat{\theta}_{c.m.} = 90^0),$$

where, $\Delta U/U$ represents U quark polarization, $\Delta V/V$ gluon polarization, and $\hat{A}_{LL}^{UV}$ in $U^{\uparrow}V^{\uparrow} \rightarrow U\gamma$ at $\hat{\theta}_{c.m.} = 90^0$.

One can relate[8] $\Delta U(X_{\perp})/U(X_{\perp})$, which can be obtained from A_1 values.[9,10]

$$\hat{A}_{LL}^{UV}\ (\hat{\theta}_{c.m.} = 90^0) = +\ 0.6 \text{ by QCD.}$$

Thus, we will be able to determine $\Delta V(X_{\perp})/V(X_{\perp})$ by measuring $A_{LL}\ (x_F = 0,\ X_{\perp})$.

Table I

Parameters and Characteristics of the CEMC

-	Lead-glass cell dimensions	38 x 38 x 450 mm^3
-	Type of glass	F-8
-	Total number of cells	2016
-	Working area and weight of the spectrometer	$0.8m^2$, 2.5 t
-	Photomultiplier	FEU-84-3
-	Accuracy in measuring photon coordinate	
	At 25 GeV	$\pm$ 2 mm
	At 100 GeV	$\pm$ 1 mm
-	Photon energy resolution	
	At 25 GeV	$\pm$ 2.5%
	At 100 GeV	$\pm$ 1.5%
-	Mass resolution for decaying particles	$\pm$ 8%
-	Time resolution	40 nsec gate

Table II

Estimates of Total Number of Events and Corresponding Statistical Errors In A_N ($pp \rightarrow \pi^\circ x$) for 1000 Hours Use of the Beam Time

$p_\perp$ (GeV/c)	$x_\perp$	Δx_F	$\Delta p_\perp$	Number of Events	ΔA_N %
2 - 2.5	0.21	0.1	0.5	7.2×10^6	0.10
2.5 - 3	0.26	0.1	0.5	1.1×10^6	0.24
3 - 4	0.31	0.125	1.0	2.6×10^5	0.45
4 - 5	0.41	0.15	1.0	1.4×10^4	2.0
5 - 6	0.52	0.20	1.0	9.3×10^2	8.1

Table III

Estimates of Total Number of Events and Corresponding Statistical Errors In A_N ($pp \rightarrow \gamma x$) for 1000 Hours Use of the Beam Time

$p_\perp$ (GeV/c)	$x_\perp$	Δx_F	$\Delta p_\perp$	Number of Events	ΔA_N %
2 - 2.5	0.21	0.1	0.5	3.6×10^5	0.35
2.5 - 3	0.26	0.1	0.5	5.5×10^4	1.4
3 - 4	0.31	0.125	1.0	1.3×10^4	2.0
4 - 5	0.41	0.15	1.0	1.4×10^3	7.5

Table IV

Estimates of Statistical Errors in A_{LL} $(pp \rightarrow \pi^{\circ}x)$ Assuming 1000-Hour Use of the Beam Time

$p_{\perp}$ (GeV/c)	$\Delta\ p_{\perp}$	Number of Events	ΔA_{LL}%
2.0 - 2.5	0.5	$1.6 \cdot 10^7$	0.15
2.5 - 3.0	0.5	$2.3 \cdot 10^6$	0.40
3.0 - 4.0	1.0	$5.5 \cdot 10^5$	1.0
4.0 - 5.0	1.0	$3.0 \cdot 10^4$	4.0

Table V

Estimates of Statistical Errors in A_{LL} $(pp \rightarrow \gamma x)$ Assuming 1000-Hour Use of the Beam Time

$p_{\perp}$ (GeV/c)	$\Delta\ p_{\perp}$	n	ΔA_{LL}%
2.0 - 2.5	0.5	$8.0 \cdot 10^5$	0.8
2.5 - 3.0	0.5	$1.1 \cdot 10^5$	2.7
3.0 - 4.0	1.0	$2.8 \cdot 10^4$	4.0
4.0 - 5.0	1.0	$3.0 \cdot 10^3$	12

April 28, 1989

Addendum to P-678 Update (March 31, 1989)

Identification of Direct-γ Events (page 6)

We have the following latest simulation results which are somewhat different from those described in the earlier update. (Figure 5 is incorrect and the associated conclusion is modified as follows: surrounding calorimeter is necessary). However, the new results do not change the rate and error estimate (page 10) for $p_{\perp} > 3$ GeV/c.

In Figure A, the ratio of direct γ/π° is shown together with various backgrounds/π° when the width of the surrounding calorimeter is 30cm. In Fig. B the signal (direct γ) to noise (total background) ratio is shown with respect to $p_{\perp}$. Backgrounds shown in Figure A are:

i) One γ from $\eta \to \gamma\gamma$ misses the detector

ii) One γ from $\pi^{\circ} \to \gamma\gamma$ misses the detector

iii) One γ from π° is below threshold (0.5 GeV) for detection

iv) One γ from η is below threshold

v) Others; one γ converted in the target, neutral hadrons such as n, $\bar{n}$ closely spaced two γ's from π°, etc.

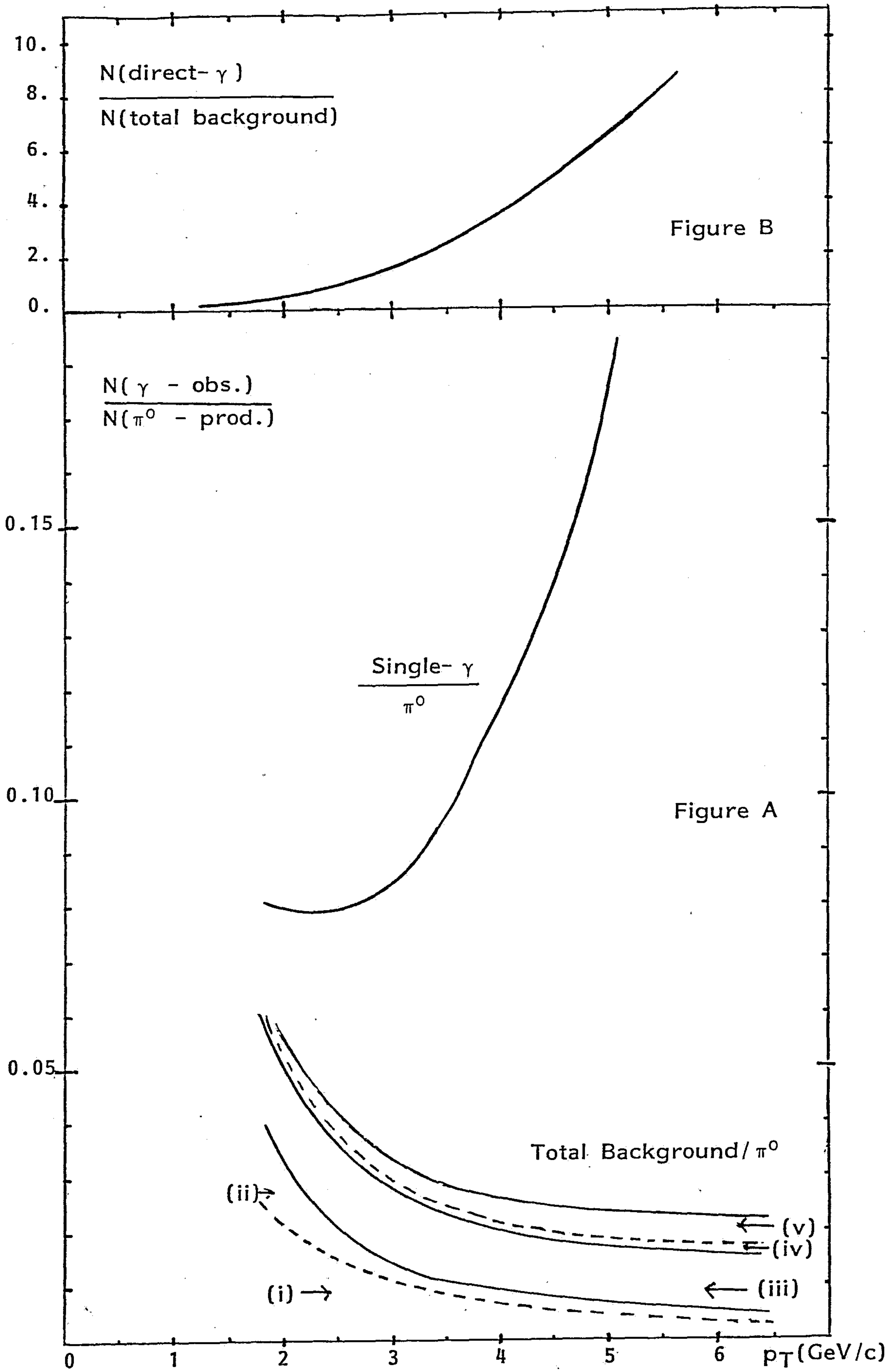

10.
8.
6.
4.
2.
0.
N(direct- γ) / N(total background)
Figure B
N(γ - obs.) / N(π⁰ - prod.)
0.15
0.10
0.05
Single- γ / π⁰
Figure A
Total Background/ π⁰
(ii)
(i)
(iii)
(iv)
(v)
0
1
2
3
4
5
6
pT(GeV/c)